Simulation of nuclear burning in astrophysics

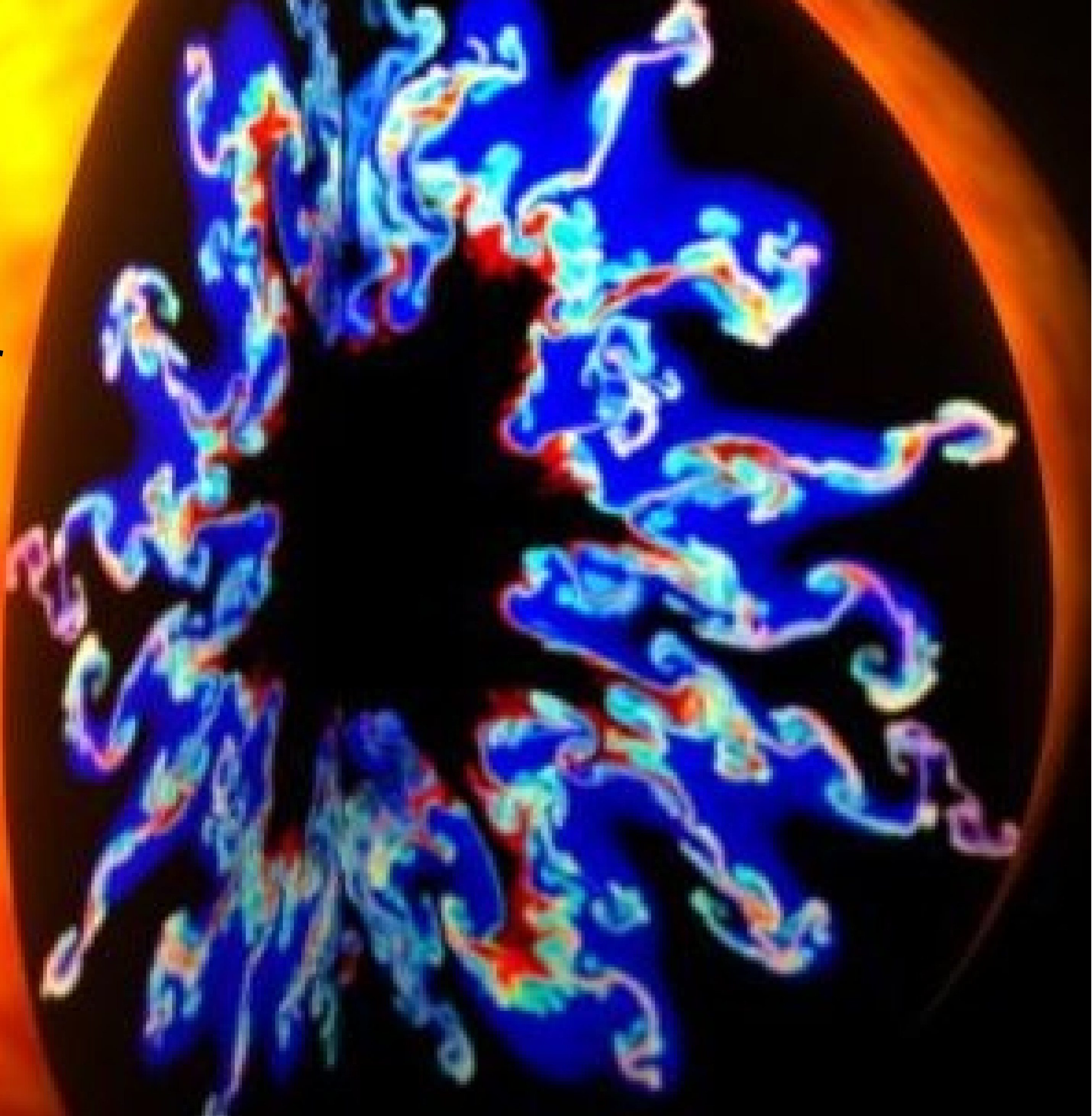

EMMI-JINA Workshop,
GSI, Oct. 13, 2012

Ewald Müller, Max-Planck-Institut für Astrophysik

Some Basic Hydrodynamics

Hydrodynamic equations are derivable from

microscopic kinetic equations (Liouville, Boltzmann)

under two assumptions

(i) microscopic behaviour of single particles can be neglected $(\lambda_{fmp} \ll L)$

(ii) forces between particles do saturate (short range forces!)

---> gravity must be treated as external force!

hydrodynamic approximation holds

--> **set of conservation laws**

simplest case: single, ideal, non-magnetic fluid; no external forces

mass: $$\frac{\partial \varrho}{\partial t} + \nabla \cdot (\varrho \vec{v}) = 0$$

momentum: $$\frac{\partial \varrho \vec{v}}{\partial t} + \nabla \cdot (\varrho \vec{v} \vec{v} + p \underline{\underline{I}}) = 0$$

energy: $$\frac{\partial \varrho E}{\partial t} + \nabla \cdot ([\varrho E + p] \vec{v}) = 0$$

hyperbolic system of PDEs

hydrodynamic approximation holds

general case: additional equations and/or

additional source terms

describe effects due to

- viscosity (*e.g.,* accretion disks)
- reactions (*e.g.,* nuclear burning, non-LTE ionization)
- conduction (*e.g.,* cooling of WD & NS; ignition of SNe Ia)
- radiation transport (*e.g.,* stars: photons; CCSNe: neutrinos)
- magnetic fields (*e.g.,* stars, jets, pulsars, accretion disks)
- self-gravity (stars, galaxies, Universe)
- relativity (jets, NS, BH, GRB)

viscous self-gravitating flow

mass:

$$\frac{\partial \varrho}{\partial t} + \nabla \cdot \left(\varrho \vec{v} \right) = 0$$

momentum:

$$\frac{\partial \varrho \vec{v}}{\partial t} + \nabla \cdot \left(\varrho \vec{v} \vec{v} + p \underline{\underline{I}} - \underline{\underline{\pi}} \right) = -\varrho \nabla \Phi$$

energy:

$$\frac{\partial \varrho E}{\partial t} + \nabla \cdot \left[\left(\varrho E + p \right) \vec{v} + \vec{h} - \underline{\underline{\pi}} \vec{v} \right] = -\varrho \vec{v} \nabla \Phi$$

Poisson equation

$$\Delta \Phi = 4 \pi G \varrho$$

Astrophysical applications:

- viscosity & heat conduction often negligibly small
  (except in shock waves)

  --> inviscous Euler eqs instead of viscous Navier-Stokes eqs are solved

- numerical methods posses numerical viscosity
  (depending on grid resolution)

  --> strange situation:

  One tries to solve inviscous Euler eqs, but instead solves a viscous variant, different from Navier-Stokes eqs !!

hydrodynamic equations are incomplete

(closure relation missing)

---> equation of state required to close system

$$p = p(\varrho, T) \, , \quad \varepsilon = \varepsilon(\varrho, T)$$

discontinuous solutions of Euler equations exist

(weak solutions: shocks, contact discont.)

---> conservation laws in integral form

jump conditions (Rankine-Hugoniot)

flows characterizable by dimensionless numbers

Reynolds number: $Re = uL/\nu$ (ν kinematic viscosity)

measures relative strength of inertia & dissipation; often very large in astrophysics ($>10^{10}$)

for all flows there exists a critical Reynolds number,

above critical Reynolds number flow becomes turbulent
---> Large Eddy Simulations (for star)

Prandtl number: $Pr = \nu/\kappa$ (σ: conductivity)

measures relative strength of dissipation & conduction

The Art of Computational Fluid Dynamics

Hydrodynamic equations:

non--linear system of 1^{st} order PDEs

one way to solve equations:

discretization in space & time

PDEs ---> set of coupled algebraic eqs

finite difference (FD), finite volume (FV), method of lines (MOL)

introduces unavoidable errors

--> It is crucial to use methods, which minimize the errors!

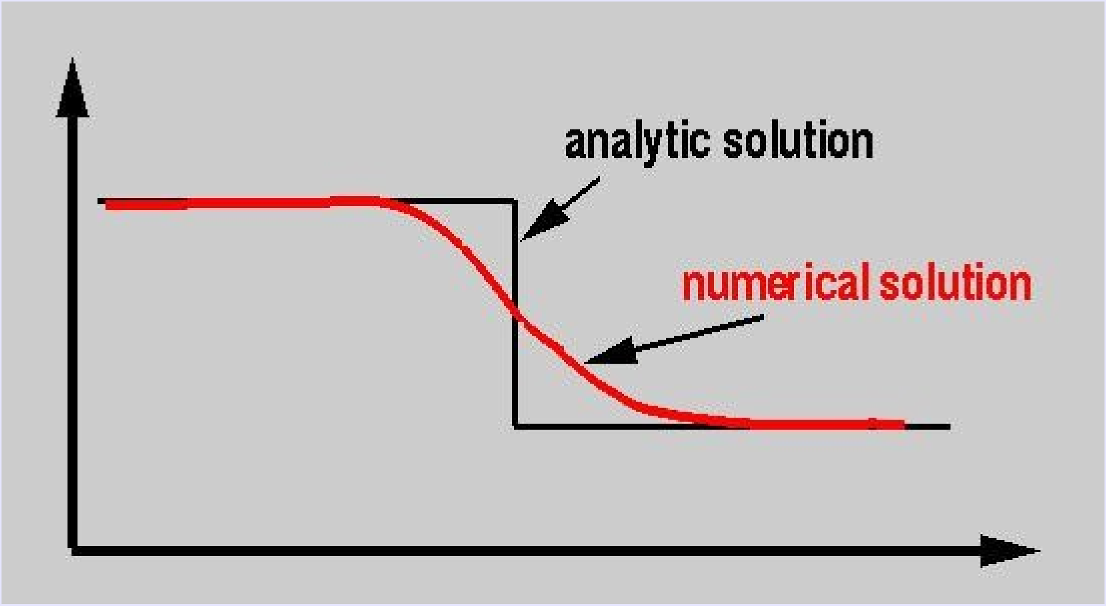

numerical diffusion

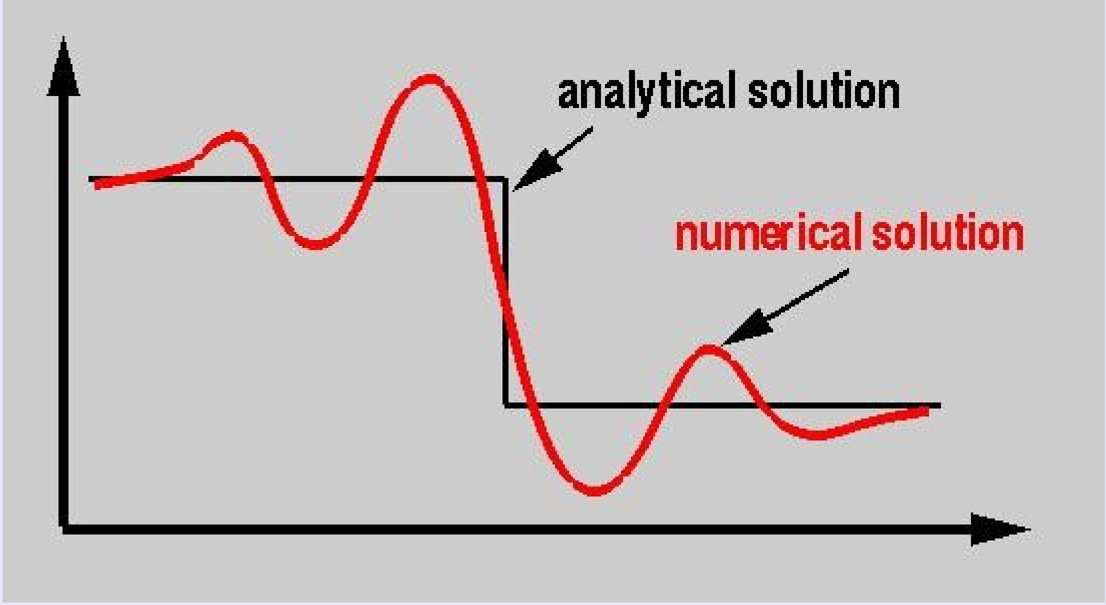

numerical dispersion

HD equations can be formulated with respect to
two distinct classes of coordinate systems

Eulerian <===> fixed coordinates (time independent)

disadvantage: :numerical diffusion
due to nonlinear advection terms (***v*** *grad*)

Lagrangian <===> comoving coordinates

(moving with the fluid/gas)

advantage: no numerical diffusion of mass, etc

disadvantage: grid tangling (in case of shear or vortex flow)

--> rezoning required which causes
numerical diffusion

--> major advantage lost!

===> Eulerian coordinates are to be preferred for multidimensional problems

but special efforts are necessay to minimize the inevitable numerical diffusion

---> use more accurate, high-order numerical schemes

alternative: free-Lagrange methods

i.e. grid free methods, where gradients are evaluated without the use of any grid

---> no grid tangling, no rezoning

most commonly used variant in astrophysics:
Smoothed Particle Hydrodynamics

Finite volume schemes

- quasi-linear hyperbolic system of (1D) conservation laws for state vector U

$$U_t(x,t) + F_x[U(x,t)] = 0$$

- or with the Jacobian A(u) ≡ ∂F/∂U of the flux vector F(U)

$$U_t + A(U) \cdot U_x = 0$$

- integration over finite (1D spatial control) volume

$$[x_1, x_2] \times [t_1, t_2]$$

$$\int_{x_1}^{x_2} U(x,t_2)\,dx = \int_{x_1}^{x_2} U(x,t_1)\,dx - \int_{t_1}^{t_2} F[U(x_2,t)]\,dt + \int_{t_1}^{t_2} F[U(x_1,t)]\,dt$$

integral form allows proper handling of flow discontinuities!

High resolution shock-capturing methods (HRSC)

- rely strongly on hyperbolic & conservative character of HD eqs (upwind method along characteristics)

- shock-capturing ability
    * discontinuities are treated consistently & automatically
    * scheme reduces from high-order accuracy in smooth regions to 1st order accuracy at discontinuities

- usually based on solution of local Riemann problems (discontinuous initial value problem) at zone interfaces e.g., piecewise constant

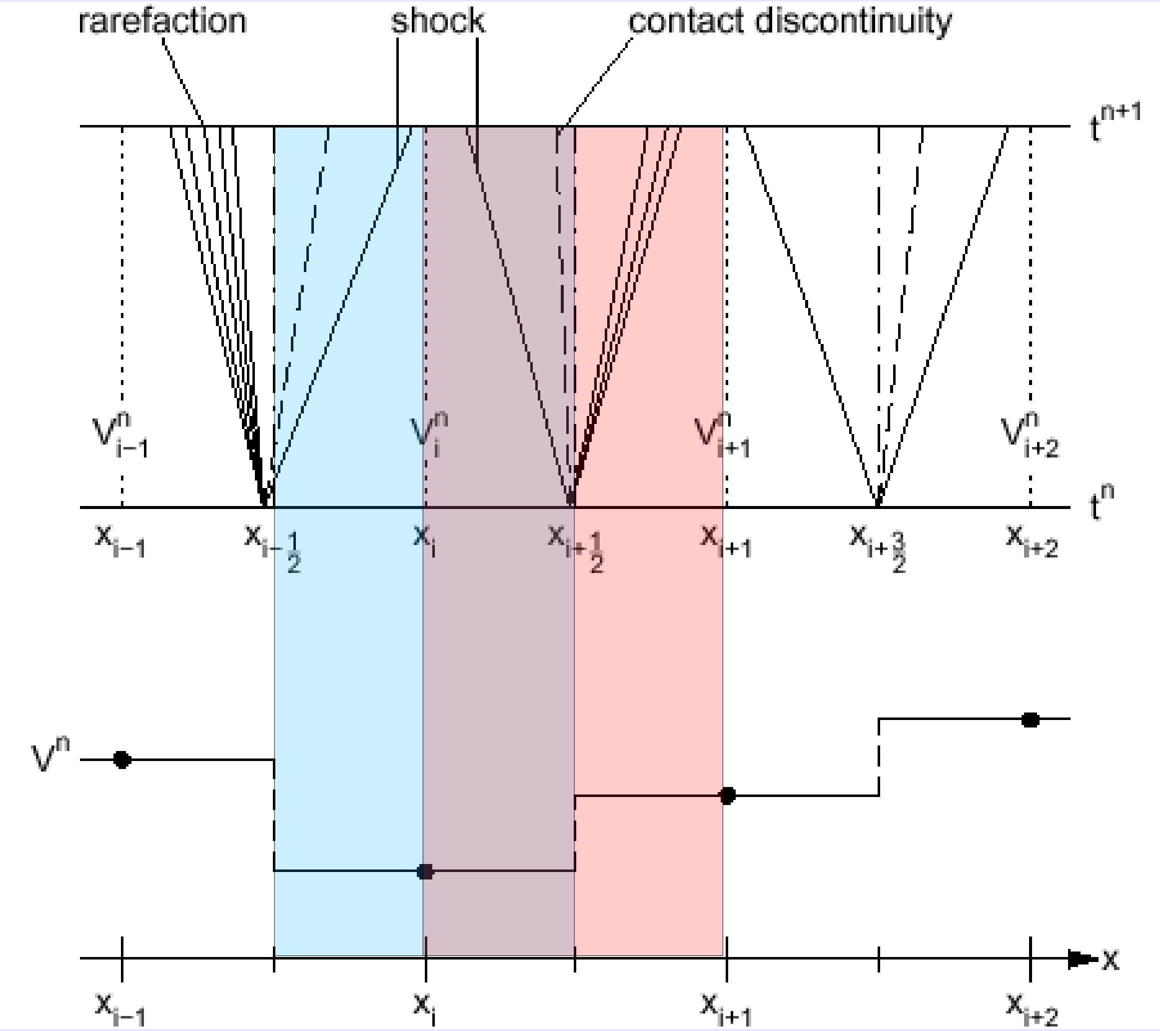

upwind schemes

numerical flux from exact or approximate solution of local Riemann problems (spectral information, i.e. Jacobian required)

central schemes

smooth numerical flux at cell centers by quadrature (averaging over Riemann fan)

proto-types: 1st order Godunov (upwind), Lax-Friedrichs (central)

non-oscillatory higher-order extensions of both classes exist!

Handling discontinuities

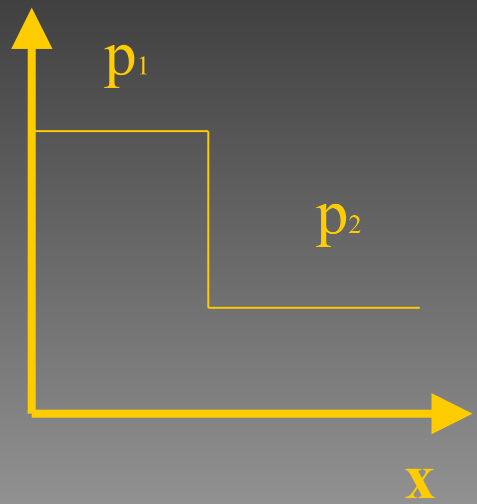

Example of a problem with discontinuous initial conditions

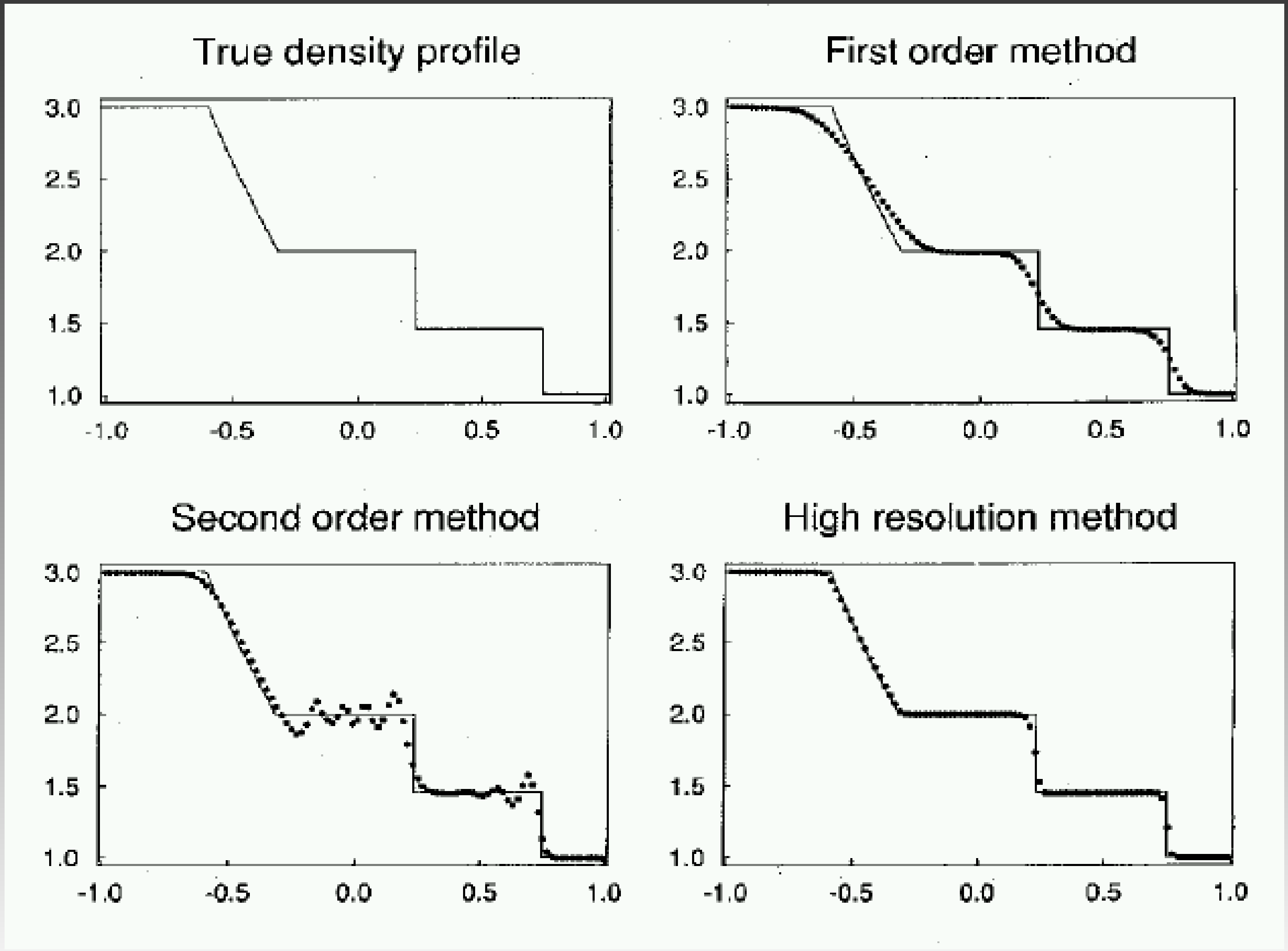

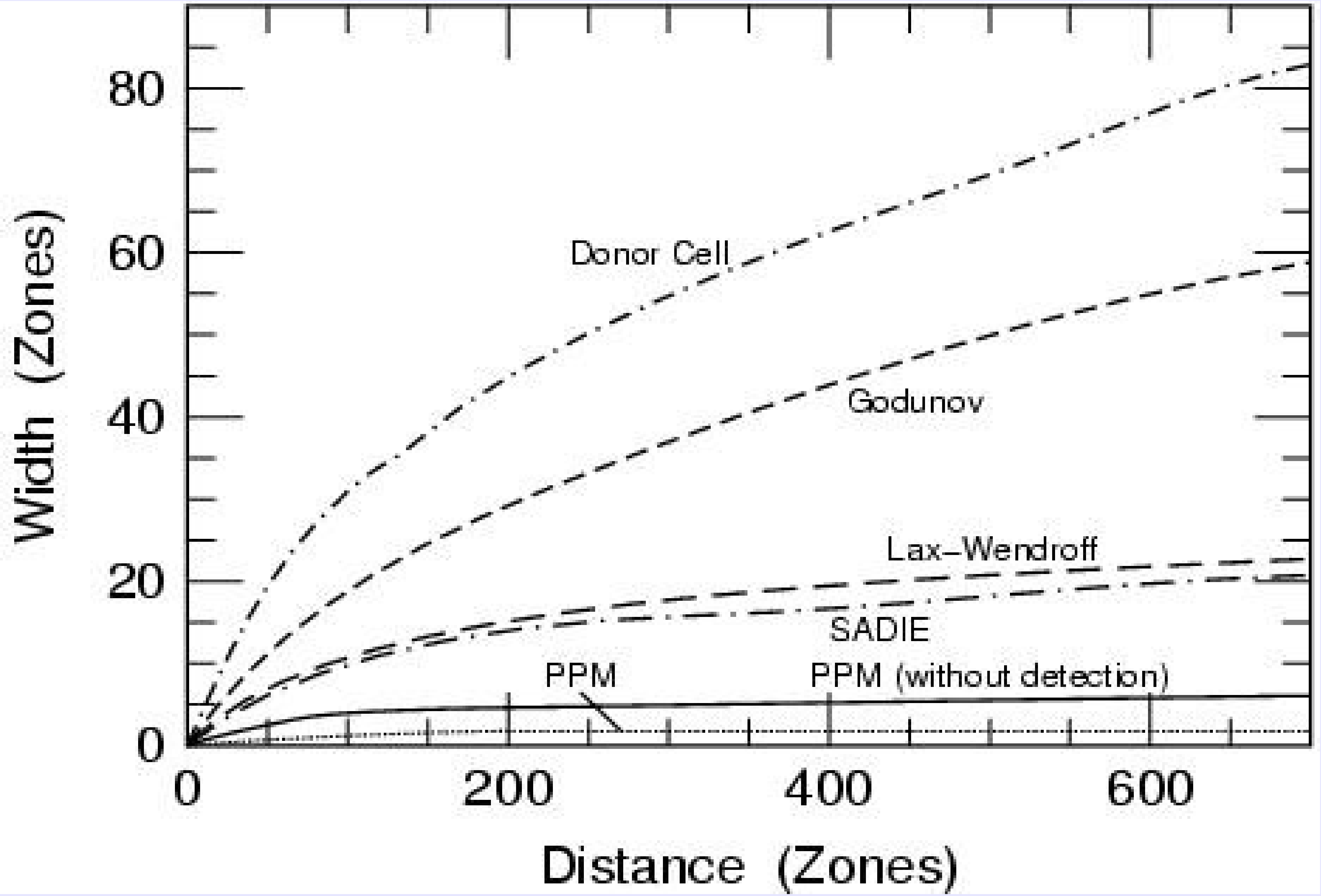

diffusivity of various finite volume methods

Sod's shock tube test problem (N=400, CFL=0.3)

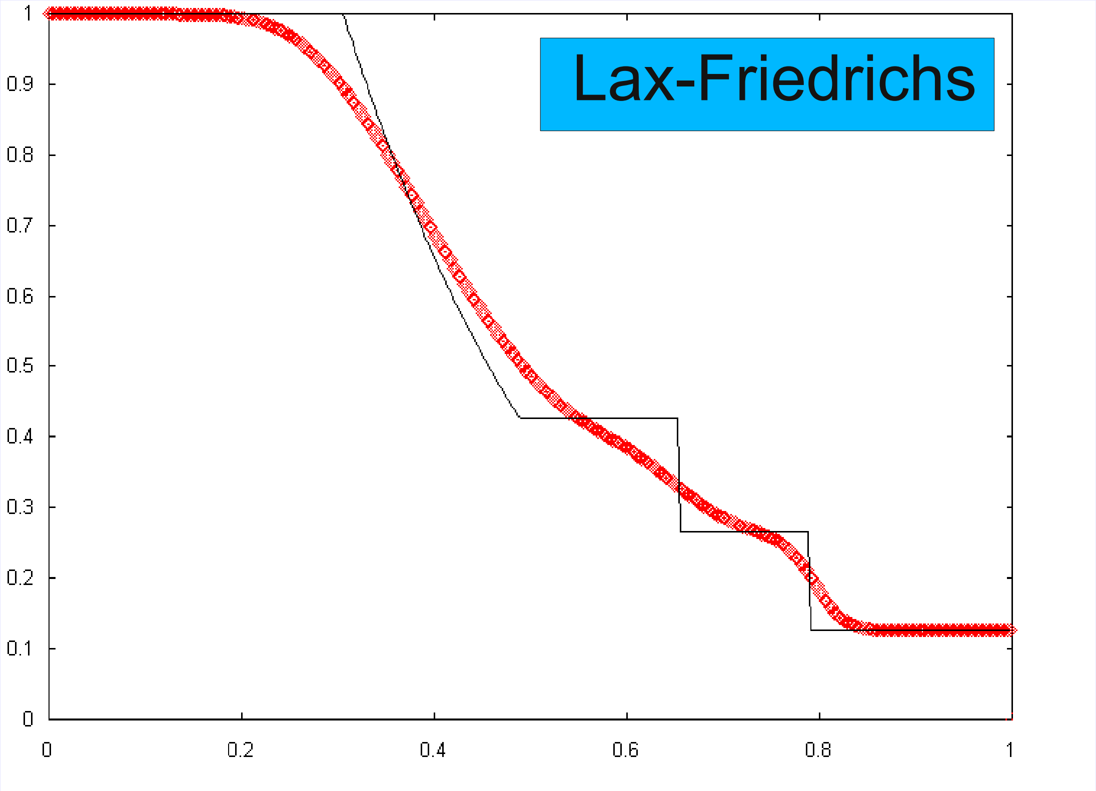

from A.Serrano

1st order central difference scheme

simple, but very diffusive everywhere

Sod's shock tube test problem **(N=400, CFL=0.3)**

diffusion

large diffusion

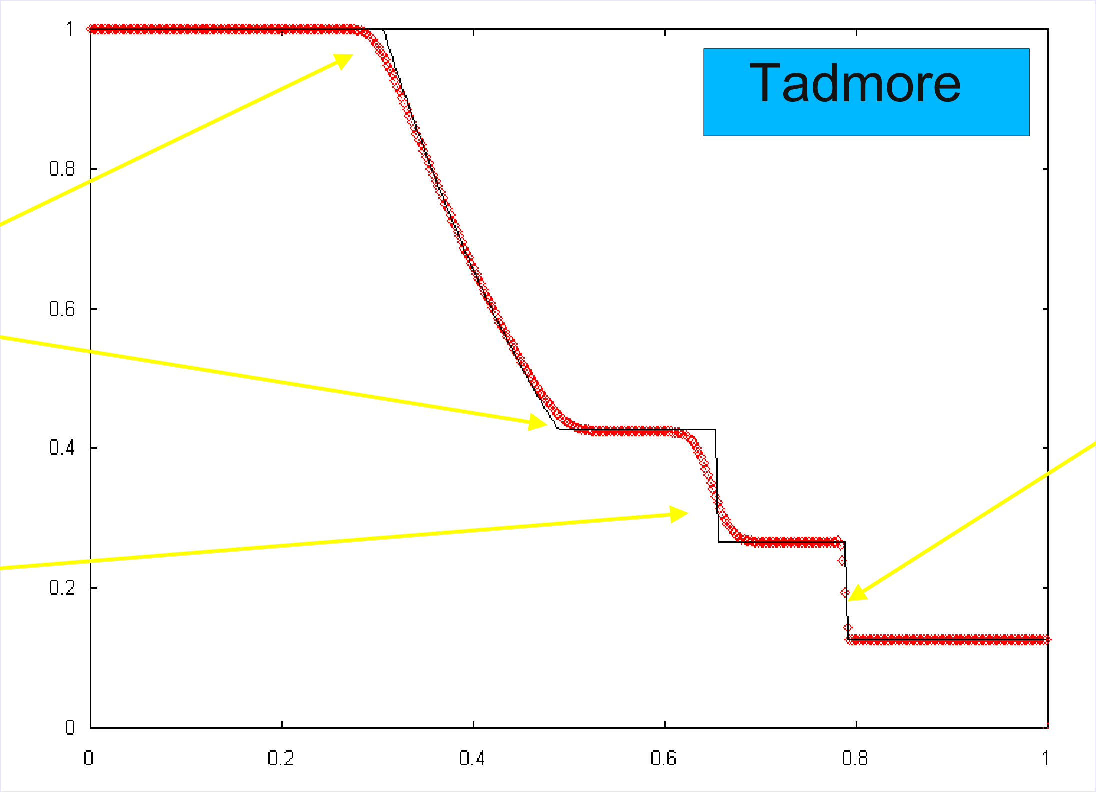

3 cells in the shock

from A.Serrano

2nd order central difference scheme

good at shocks, very diffusive at contacts

Sod's shock tube test problem (N=400, CFL=0.3)

very good resolution

small undershoots

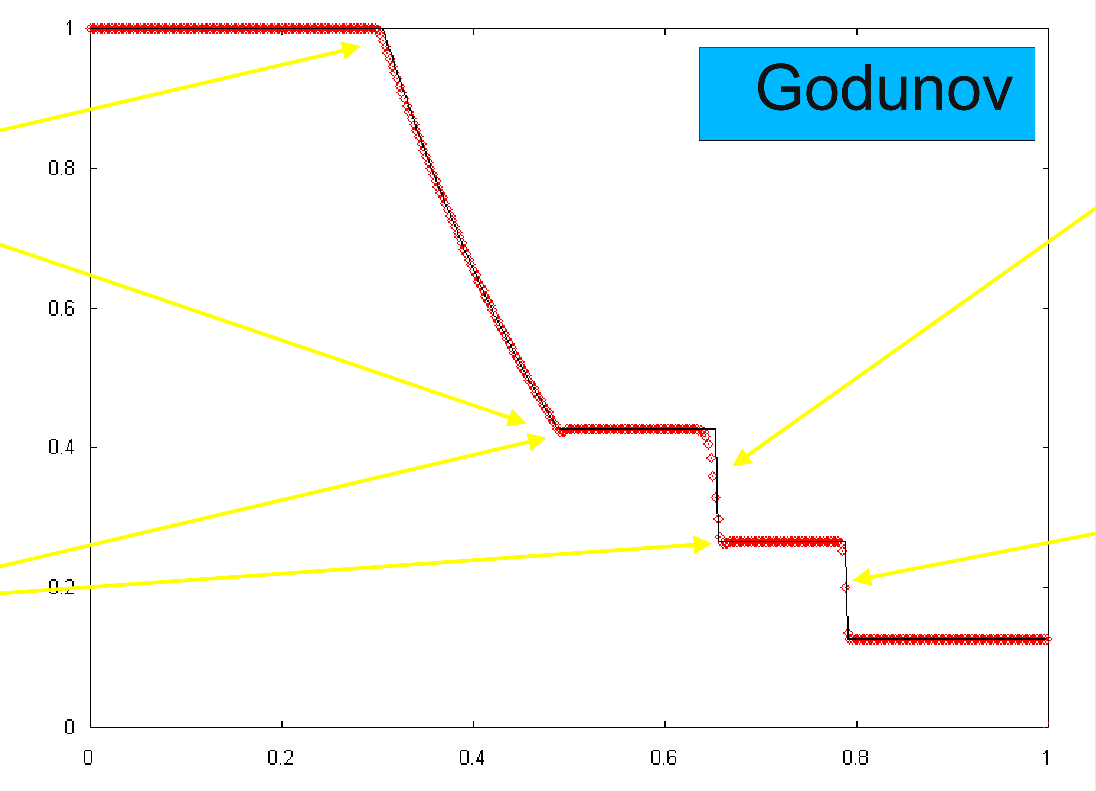

very well resolved contact

3 cells in the shock

from A.Serrano

Riemann solver, 1st order reconstruction

accurate description of all wave structures

<u>Be aware:</u> even exact Riemann solvers have flaws!

(Quirk 1994)

<u>Odd-even decoupling</u> when simulating grid-aligned.shocks with exact Riemann solvers and directional splitting (cross dissipation missing!)

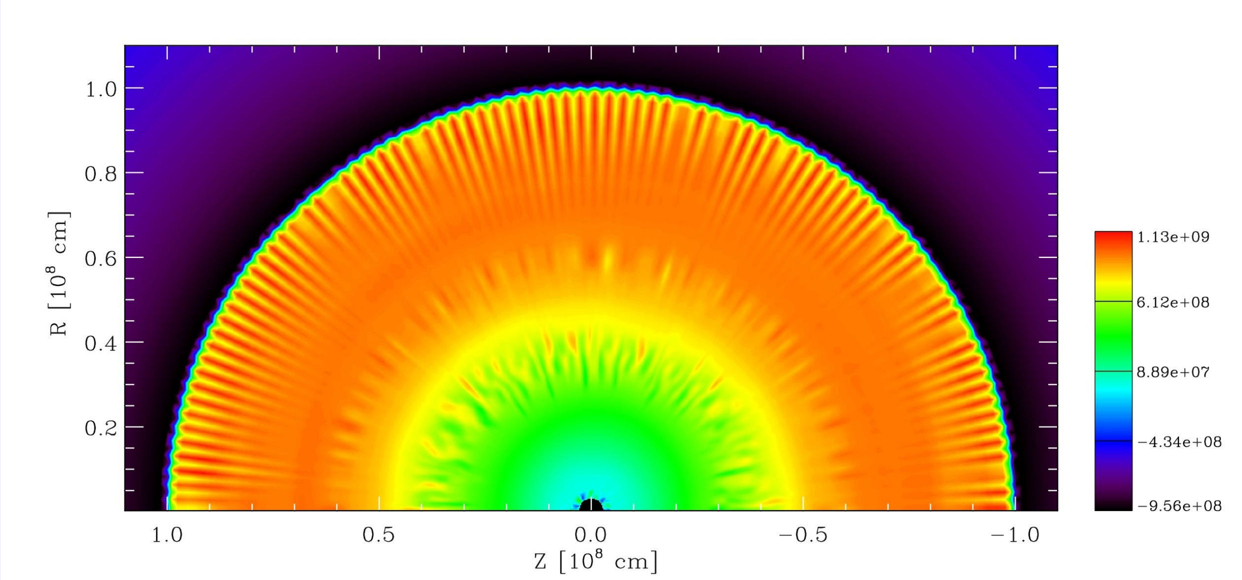

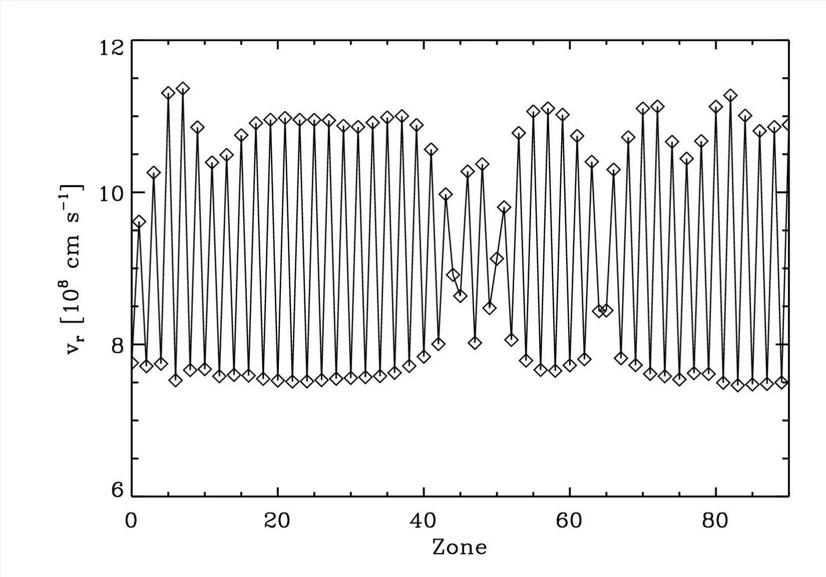

early neutrino heating phase in a core collapse supernova simulation

Simulating multi-dimensional flow

- neutrino hot bubble entropy <u>with</u> 'sticks'

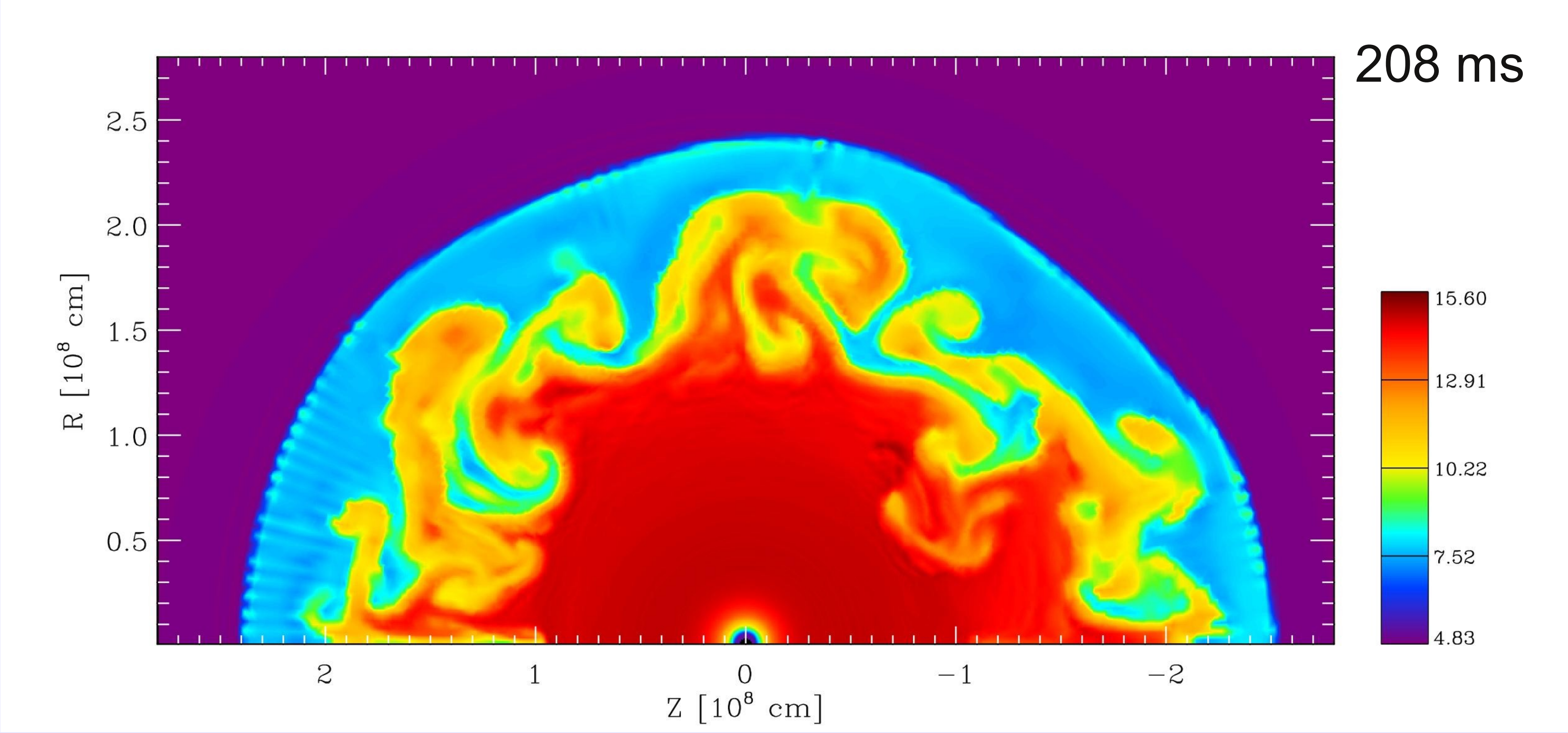

Simulating multi-dimensional flow

- neutrino hot bubble entropy <u>without</u> 'sticks'
  ---> 40% more nickel

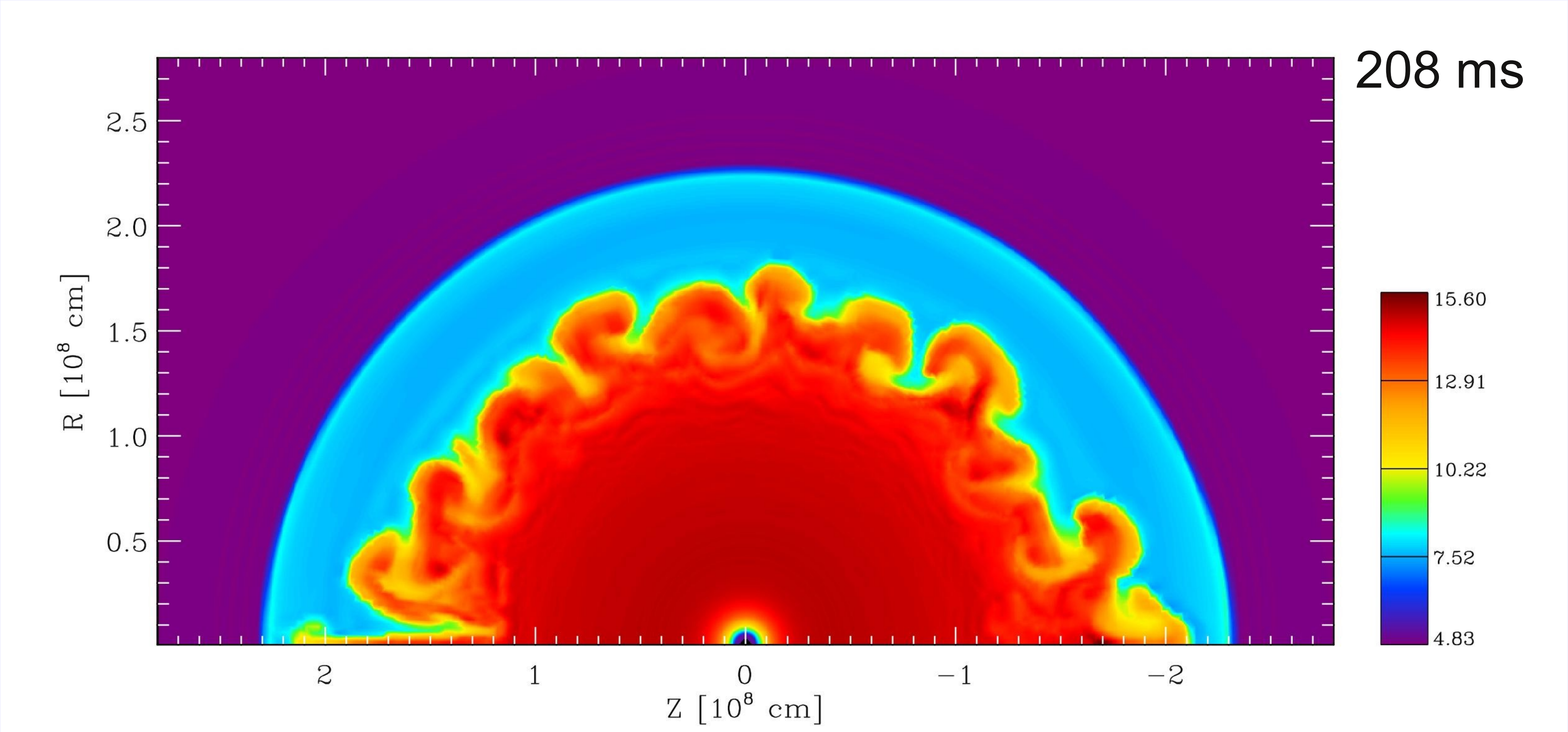

Simulation of Multi Fluid Flow

- *thermonuclear reactions* if density and temperature sufficiently high
- astrophysical situations (in particular in stellar explosions): large number of different types of reactions involved
- grouped according to number of participants in interactions:

  one-body reactions (β-decays, electron captures, photo-disintegrations),
  two-body reactions,
  three-body reactions

- notation:

  λ_j: reaction rates for 1-body

  $\langle j, k \rangle$: thermally averaged cross sections and relative velocities in the center-of-mass system for 2-body

  $\langle j, k, l \rangle$: same for 3-body

  N_A: Avogadro number

→ expression for the *change in specific abundance Y_i of species i:*

$$\dot{Y}_i = \sum_j c_i^j \lambda_i^j Y_j + \sum_{j,k} c_i^{j,k} \rho N_\mathrm{A} \langle j,k \rangle Y_j Y_k + \sum_{j,k,l} c_i^{j,k,l} \left(\rho N_\mathrm{A}\right)^2 \langle j,k,l \rangle Y_j Y_k Y_l$$

coefficients c:

$$\begin{aligned} c_i^j &= \pm N_i \\ c_i^{j,k} &= \pm \frac{N_i}{N_j! N_k!} \\ c_i^{j,k,l} &= \pm \frac{N_i}{N_j! N_k! N_l!}, \end{aligned}$$

note:

- $N_{i,j,k,l}$: number of particles participating in reaction
- factorials in denominator prevent double counts
- ± stand for particle creation/destruction

advantage of using *specific abundances*

$$Y_i = \frac{n_i}{\rho N_\mathrm{A}} :$$

values unaffected by expansion and contractions (unlike number densities n_i); changes in Y_i really require nuclear processes or mixing *nuclear reaction network*

$$\dot{Y}_i = \sum_j c_i^j \lambda_i^j Y_j + \sum_{j,k} c_i^{j,k} \rho N_\mathrm{A} \langle j,k \rangle Y_j Y_k + \sum_{j,k,l} c_i^{j,k,l} (\rho N_\mathrm{A})^2 \langle j,k,l \rangle Y_j Y_k Y_l \qquad (110)$$

- set of coupled nonlinear ODEs
- nonlinearity due to dependence of reaction rates on second or higher powers of Y_i
- stiffness due to vastly different values of Y_i and of reaction rates (may depend on high powers of T and ρ)
- nonlinearity $\rightarrow$ analytic solution virtually impossible
- numerical approach inevitable

for convenience of discussion of numerical solution strategies: rewrite (110)

$$\frac{\mathrm{d}Y_i}{\mathrm{d}t} = f_i(\rho, T, Y_1, \ldots, Y_N), \qquad (i = 1, \ldots, N, \text{ number of species})$$

numerical solution of a nuclear reaction network

$$\frac{\mathrm{d}Y_i}{\mathrm{d}t} = f_i(\rho, T, Y_1, \ldots, Y_N), \qquad (i = 1, \ldots, N, \text{ number of species})$$

- approximate left hand side by *finite difference:*

$$\frac{\mathrm{d}Y_i}{\mathrm{d}t} \approx \frac{Y_i^{n+1} - Y_i^n}{\Delta t},$$

  → finite difference scheme by evaluating f_i numerically
- simple approach:
  either at time step t^n

$$Y_i^{n+1} = Y_i^n + \Delta t\, f_i^n$$

  or at time step $t^{n+1} = t^n + \Delta t$:

$$Y_i^{n+1} = Y_i^n + \Delta t\, f_i^{n+1}.$$

  → *Euler method* for solving the ODEs: 1st-order accurate in time
- 1st variant: explicit *Forward Euler* scheme
  can be implemented in a straightforward way
  but: numerical difficulties near steady state and equilibrium solutions

numerical solution of a nuclear reaction network

- 2nd variant: the implicit *Backward Euler* method
  generally preferred
  implicit → more implementation effort: set of coupled nonlinear equations, *solved by matrix manipulation techniques*
- abbreviation: Backward Euler in *vector notation:*

$$\boldsymbol{Y}^{n+1} = \boldsymbol{Y}^n + \Delta t \boldsymbol{f}^{n+1} = \boldsymbol{Y}^n + \Delta t \boldsymbol{f}(\boldsymbol{Y}^{n+1}).$$

- expand $\boldsymbol{f}(\boldsymbol{Y}^{n+1})$ into *Taylor series* about known $\boldsymbol{f}(\boldsymbol{Y}^n)$
  retain first-order terms only (↔ Newton's method):

$$(\boldsymbol{Y}^{n+1} - \boldsymbol{Y}^n)\left(\frac{\boldsymbol{I}}{\Delta t} - \boldsymbol{J}\right) = \boldsymbol{f}(\boldsymbol{Y}^n), \qquad (111)$$

$\boldsymbol{I}$: identity matrix $I_{ij} = \delta_{ij}$
$\boldsymbol{J}$: Jacobian matrix

numerical solution of a nuclear reaction network

- $\boldsymbol{J}$: *Jacobian matrix*

$$\boldsymbol{J} = \frac{\partial f(Y^n)}{\partial Y^n}$$

represents the flow (nuclei per second) into and out of isotope

in principle, matrix completely filled
(all isotopes interact)
however: many entries very small
→ omitted

→ in practice:
sparse Jacobian matrix
(usually diagonally dominant)

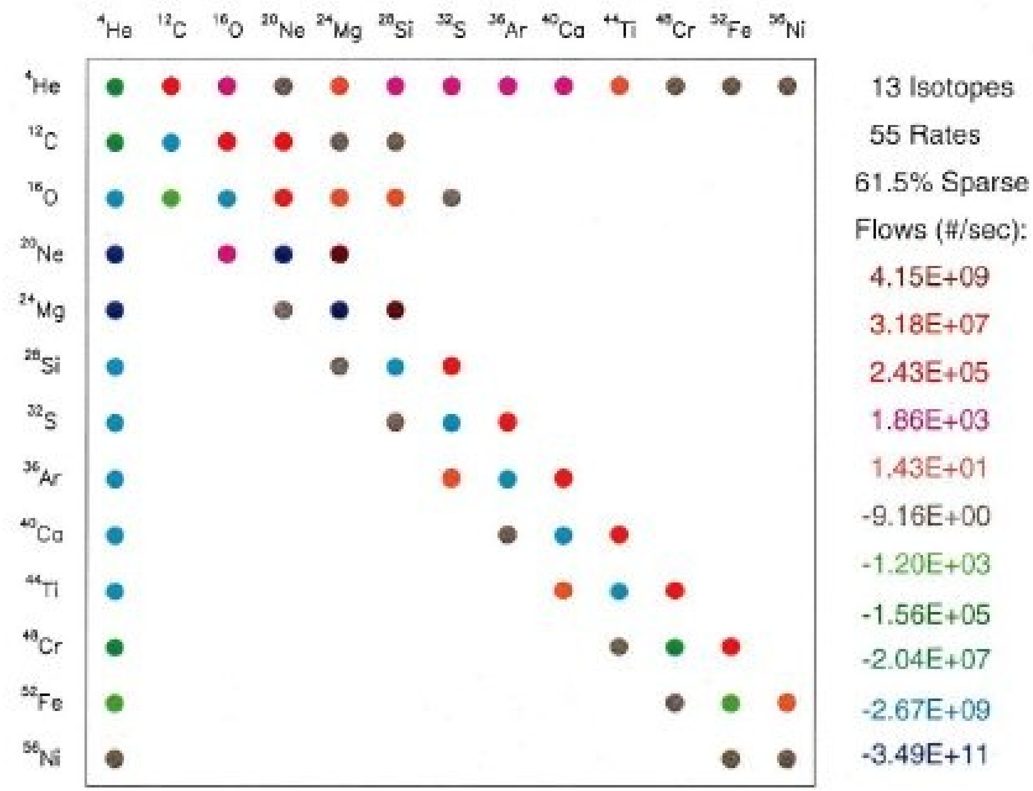

numerical solution of a nuclear reaction network

- J: *Jacobian matrix*

$$J = \frac{\partial f(Y^n)}{\partial Y^n}$$

represents the flow (nuclei per second) into and out of isotope

in principle, matrix completely filled
(all isotopes interact)
however: many entries very small
→ omitted

→ in practice:
sparse Jacobian matrix
(usually diagonally dominant)

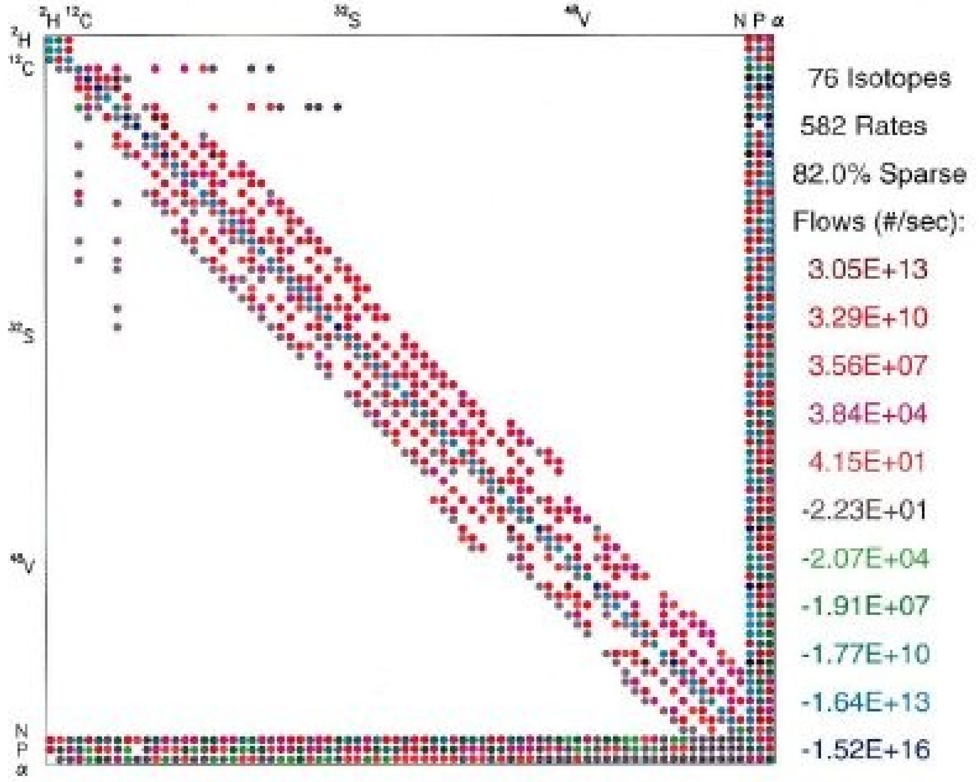

numerical solution of a nuclear reaction network

- J: *Jacobian matrix*

$$J = \frac{\partial f(Y^n)}{\partial Y^n}$$

represents the flow (nuclei per second) into and out of isotope

in principle, matrix completely filled
(all isotopes interact)
however: many entries very small
→ omitted

→ in practice:
sparse Jacobian matrix
(usually diagonally dominant)

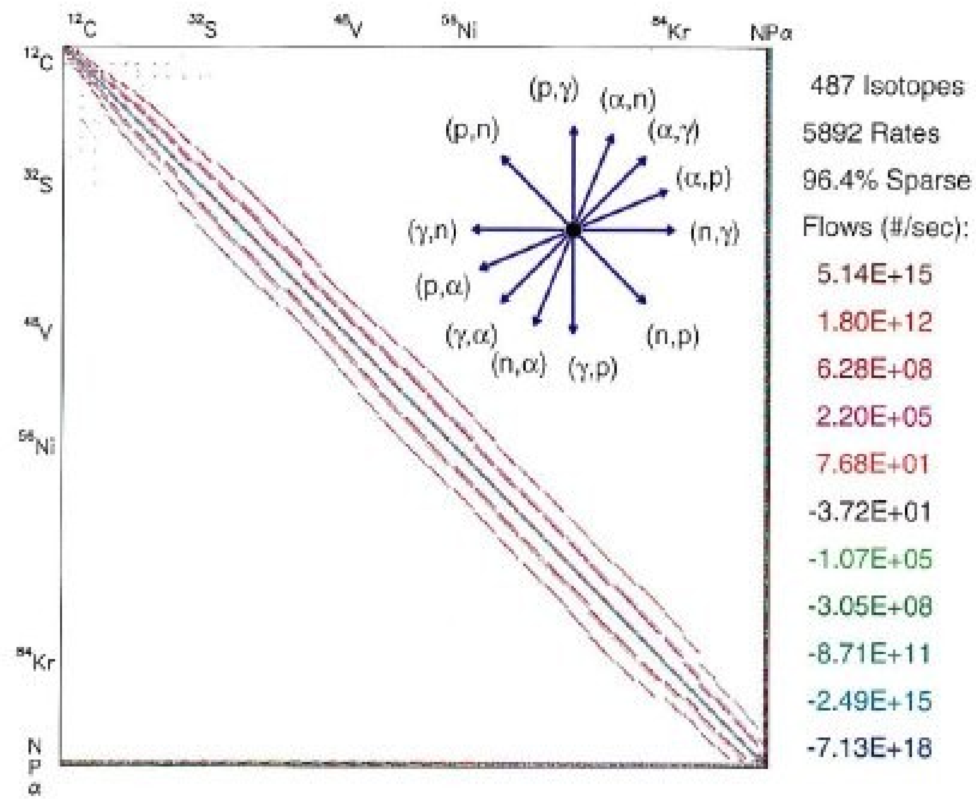

numerical solution of a nuclear reaction network

solve

$$(\boldsymbol{Y}^{n+1} - \boldsymbol{Y}^{n})\left(\frac{\boldsymbol{I}}{\Delta t} - \boldsymbol{J}\right) = \boldsymbol{f}(\boldsymbol{Y}^{n})$$

- evaluate Jacobian matrix
- evaluate $\boldsymbol{f}(\boldsymbol{Y}^{n})$
- invert matrix

$$\frac{\boldsymbol{I}}{\Delta t} - \boldsymbol{J}$$

- back substitution to determine Y^{n+1}
- matrix inversion, e.g. by linearization → *semi-implicit scheme*

Coupling hydrodynamics and reaction source terms

- *interdependencies* of hydro and reactions:
  - reactions change hydrodynamic states
    $\rightarrow$ releasing (or consuming) energy,
    convert species
  - reaction rates sensitively depend on thermodynamic state (T, ρ)
- coupling is *local in space*

reflected by *extension to the Euler equations*:

- add extra equation accounting for *species balance*

$$\frac{\partial \rho Y_i}{\partial t} = -\boldsymbol{\nabla} \cdot (\rho Y_i \boldsymbol{v}) + \rho f(Y_i) \qquad i = 1 \dots N \tag{112}$$

  $f(Y_i)$: *source term* accounting for production or destruction of species i by nuclear reactions

Coupling hydrodynamics and reaction source terms

- *energy balance* completed with *source term* $S = S(f(Y_i))$ due to nuclear energy release/consumption:

$$\frac{\partial \rho e_{\mathrm{tot}}}{\partial t} = -\nabla \cdot (\rho e_{\mathrm{tot}} \boldsymbol{v}) - \nabla \cdot (P \boldsymbol{v}) + \rho S(f) \tag{113}$$

  $\Delta m_i = (m_i - A_i m_{\mathrm{u}})c^2$: mass excess [MeV]
  m_{u}: atomic mass unit [MeV]

- energy source term $[\mathrm{erg\,cm^{-3}\,s^{-1}}]$

$$S = -9.644 \times 10^{17} \rho \sum_i \Delta m_i c^2 f_i \, \frac{\mathrm{erg}}{\mathrm{cm^3\,s^1}}$$

→ together with appropriate equations for mass and momentum conservation:

reactive Euler equations

(here without external forces, e.g. gravity)

Self-gravitating multi-dimensional multi-fluid ideal flow

$$\frac{\partial \varrho}{\partial t} + \nabla \cdot (\varrho \vec{v}) = 0$$

$$\frac{\partial \varrho \vec{v}}{\partial t} + \nabla \cdot (\varrho \vec{v} \vec{v}) + \nabla P + \varrho \nabla \Phi = 0$$

$$\frac{\partial \varrho E}{\partial t} + \nabla \cdot ([\varrho E + P] \vec{v}) + \varrho (\vec{v} \cdot \nabla) \Phi = \varrho \dot{Q}_{nuc}$$

$$\frac{\partial \varrho X_i}{\partial t} + \nabla \cdot (\varrho X_i \vec{v}) = \varrho \dot{X}_i \; , \quad \sum_i X_i = 1$$

X = Y * A

Simulations of core collapse & thermonuclear supernovae require a numerical treatment of multi-fluid flow

- Non-linear discretization of advection terms

--> $$\sum_i X_i \neq 1$$

- Consistent Multi-fluid Advection (Plewa & Müller '99)

  (a) renormalization of mass fraction fluxes

  (b) conservative species advection

  (c) contact steepening to reduce numerical diffusion

Simulating multi-fluid flow

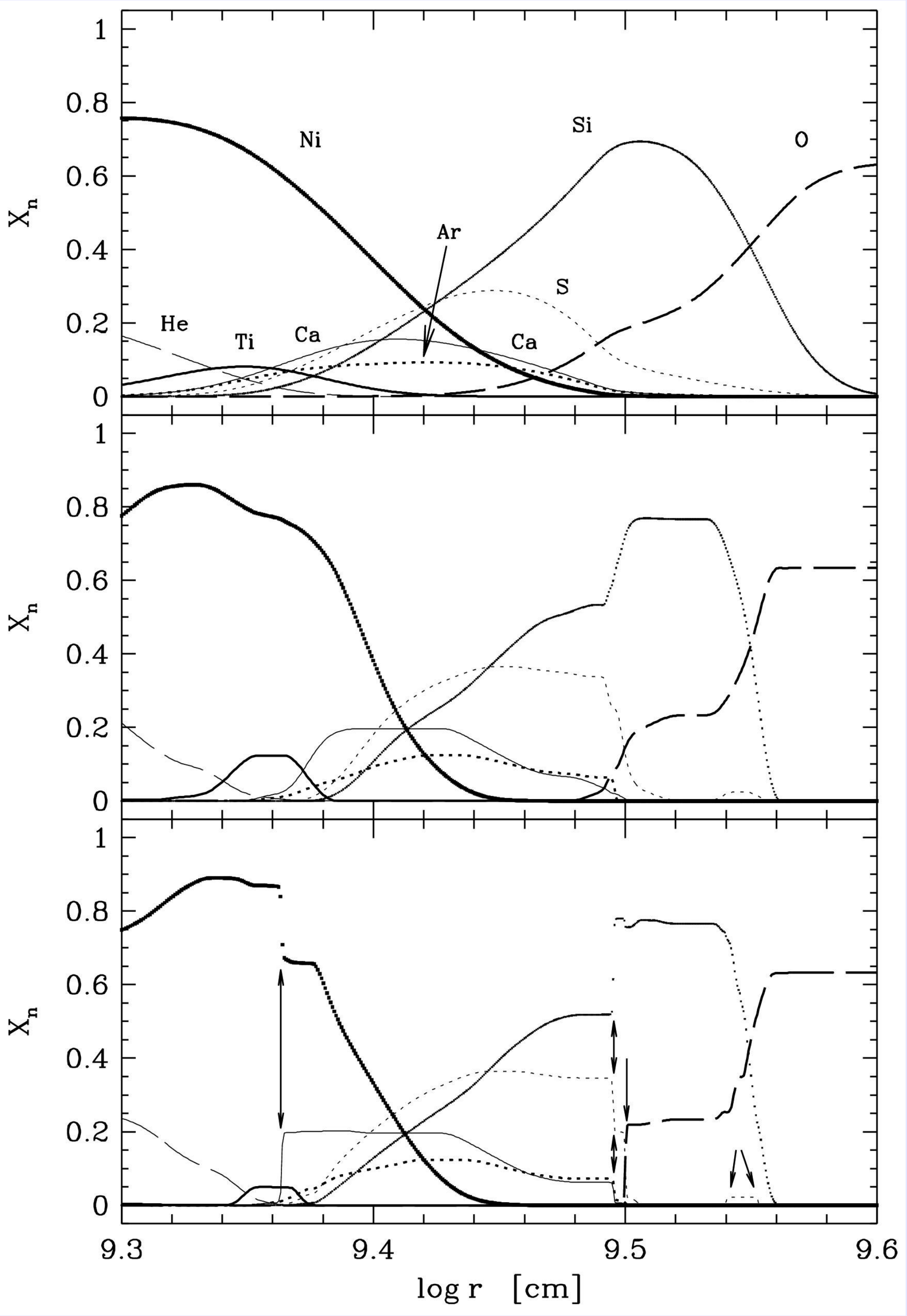

CMAZ

(total flattening)

FMA

(Fryxell, Müller & Arnett 1989)

CMA

(Plewa & Müller 2001)

Composition profiles in the ejecta of a 15 solar mass star at 3 sec

Simulating multi-fluid flow

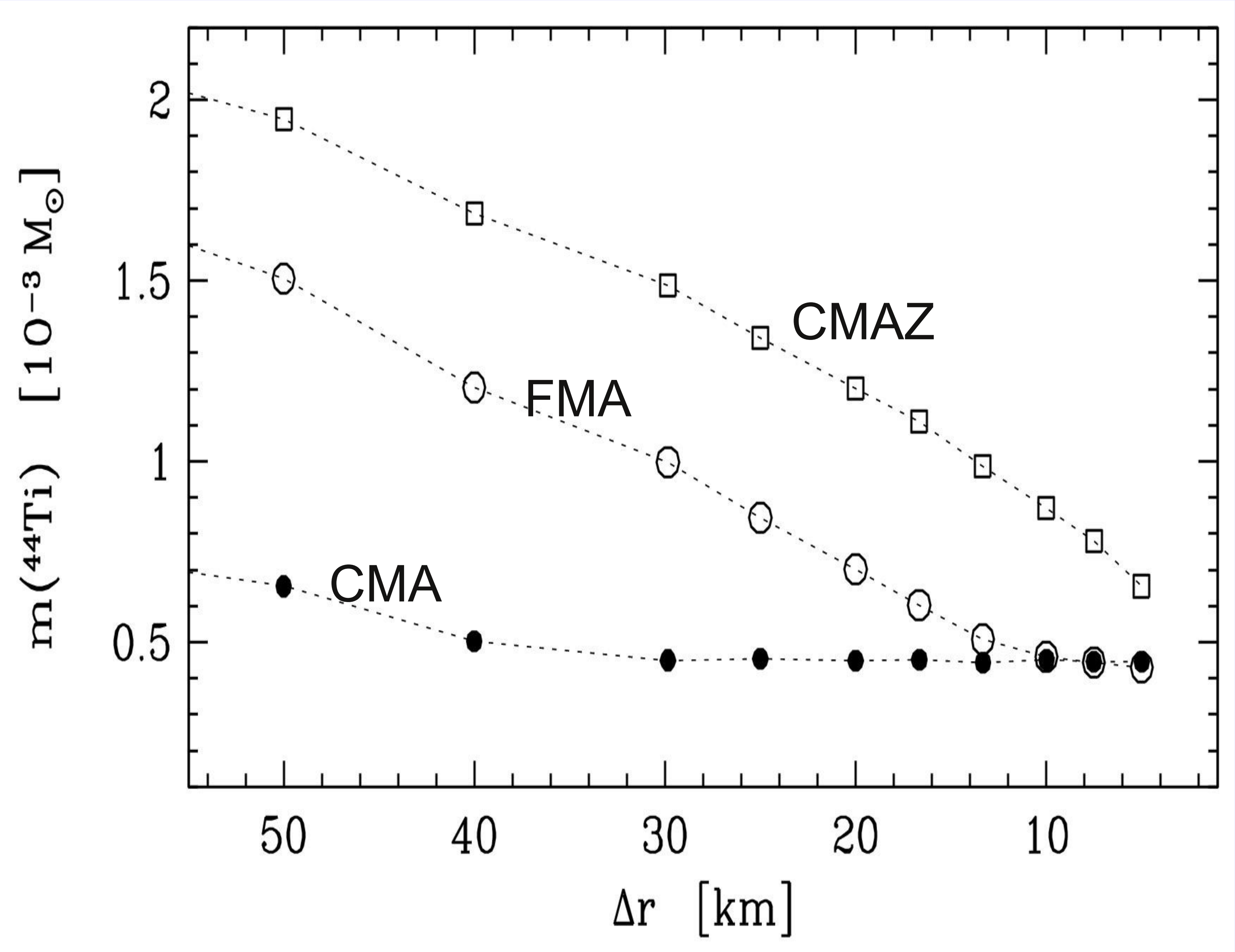

dependence of ^{44}Ti production on grid resolution

Thermonuclear burning & nucleosynthesis

- Common practice nowadays
  - * 1D: online reaction network (several 100 species)
  - * 2D/3D reduced network for energy generation + post-processing
- Multi-dimensional flows

  Lagrangian codes inappropriate

  --> Eulerian codes extended by

  marker particle method

  set of marker particles properly distributed across regions expected to burn --> advected with the flow --> (T, ρ) history recorded for post-processing

Marker particle nucleosynthesis

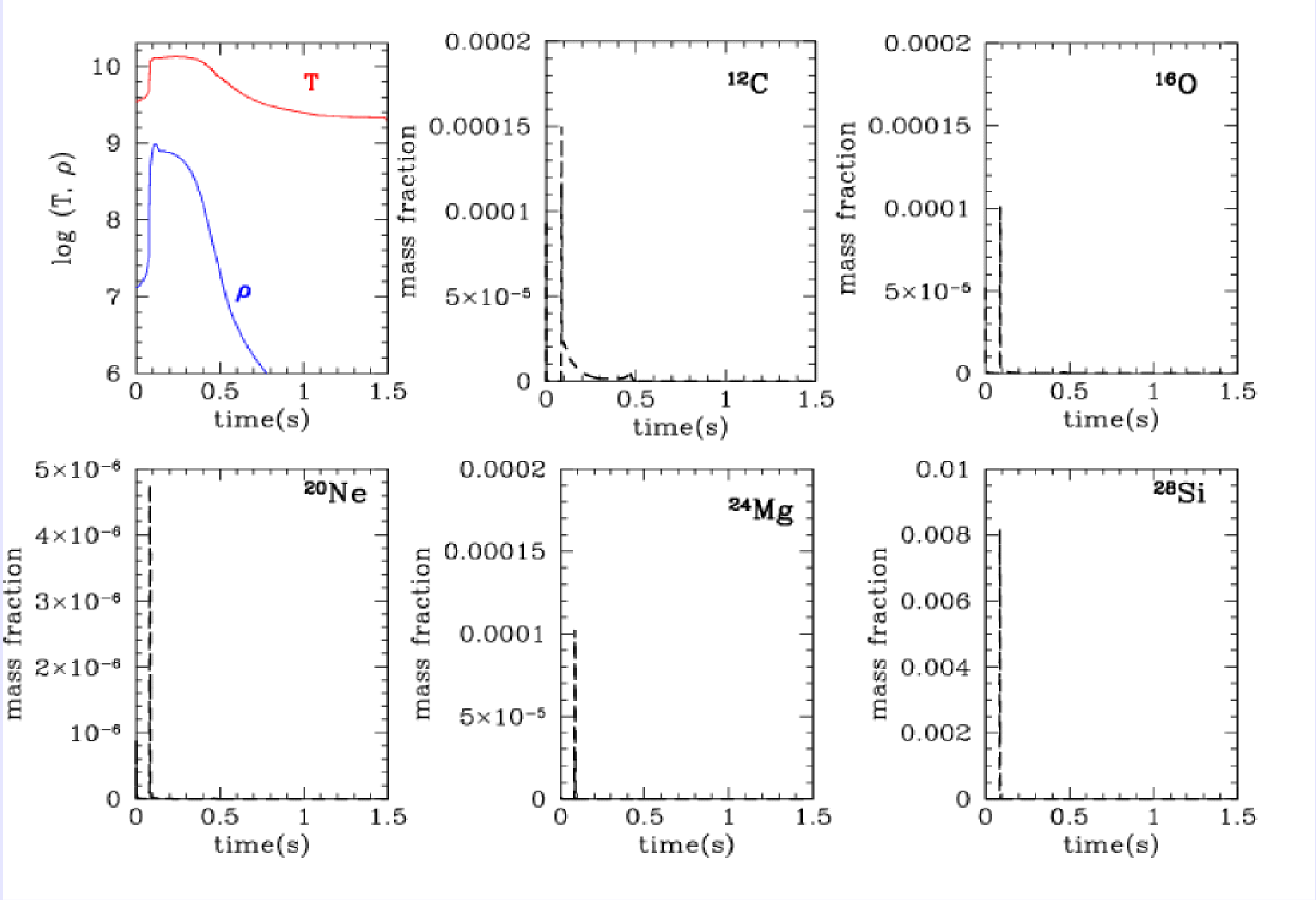

From a SNe Ia simulation using marker particles and post-processing

(Travaglio et.al 2003)

Marker particle nucleosynthesis

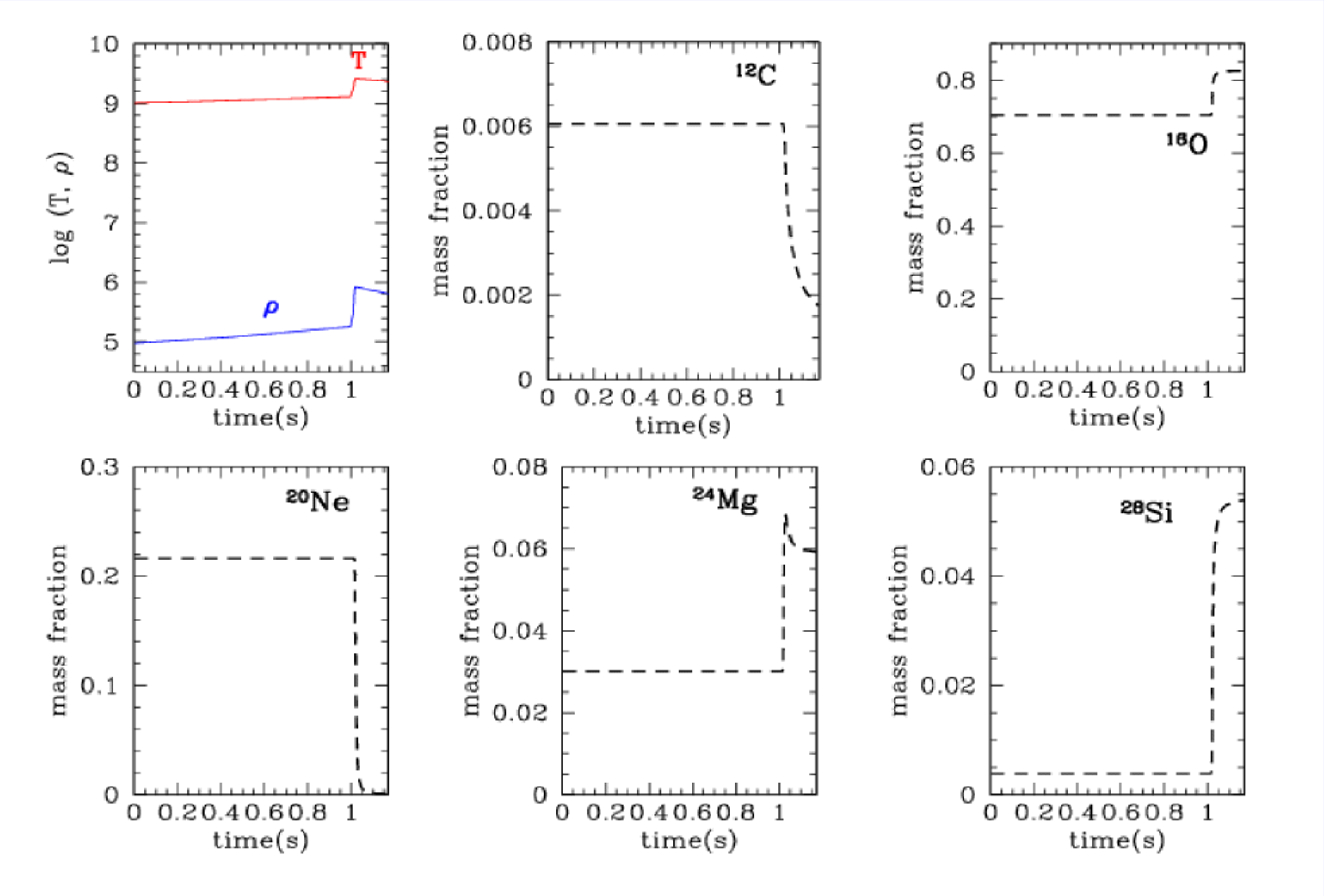

From a SNe Ia simulation using marker particles and post-processing

(Travaglio et.al 2003)

Example I

Nucleosynthesis and
Rayleigh-Taylor instabilities
in the envelopes of
core-collapse supernovae

Neutrinos & SN Explosion Mechanism

Paradigm: Explosions by the neutrino-heating mechanism, supported by hydrodynamic instabilities in the postshock layer

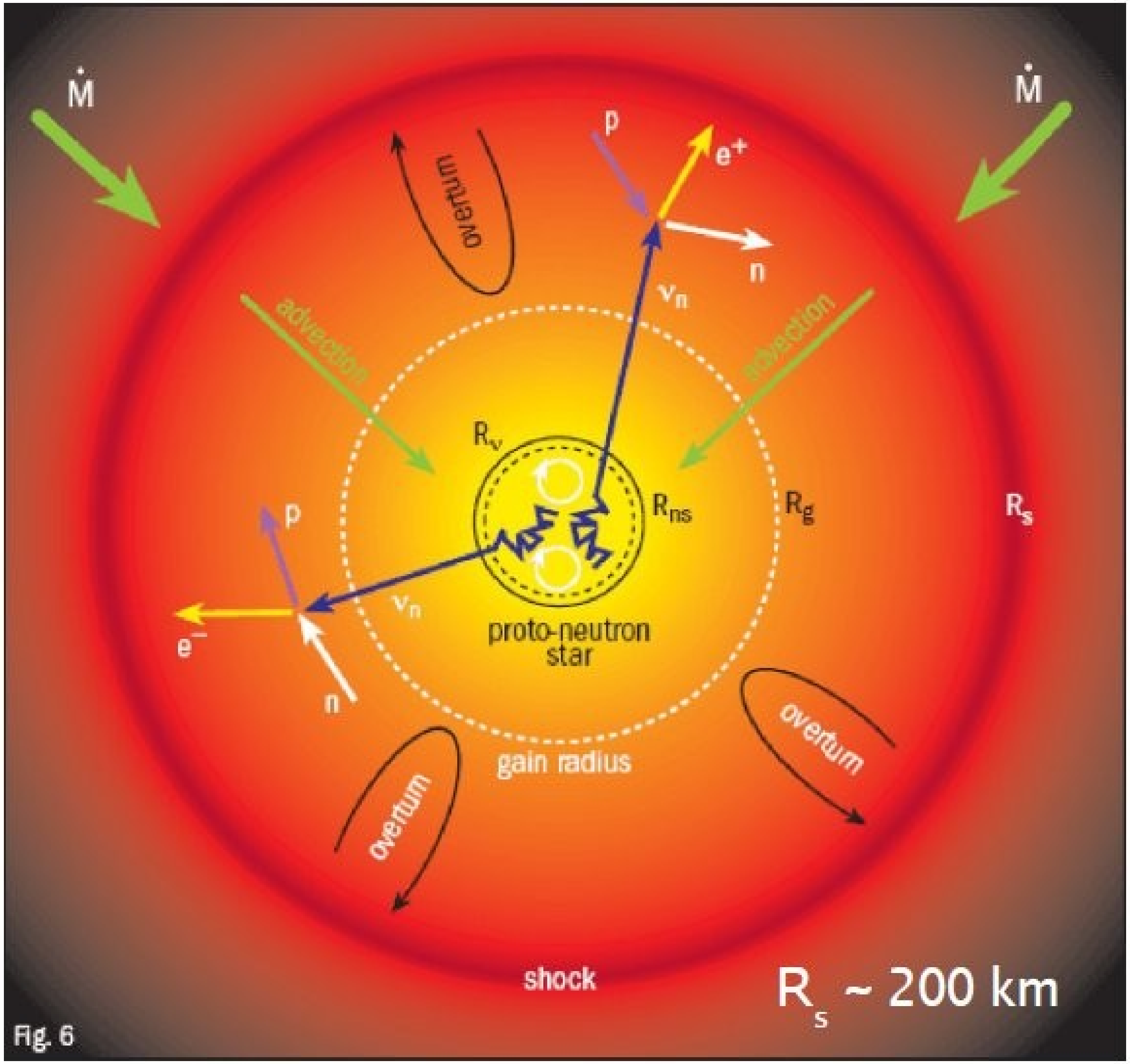

- "Neutrino-heating mechanism": Neutrinos `revive' stalled shock by energy deposition (Colgate & White 1966, Wilson 1982, Bethe & Wilson 1985);
- Convective processes & hydrodynamic instabilities support the heating mechanism (Herant et al. 1992, 1994; Burrows et al. 1995, Janka & Müller 1994, 1996; Fryer & Warren 2002, 2004; Blondin et al. 2003; Scheck et al. 2004,06,08).

courtesy of H-Th. Janka

- observations imply that non-radial flow and mixing are common in core collapse supernovae

- theoretical models based on delayed explosion mechanism predict non-radial flow and mixing due to

  - Ledoux convection inside the proto-neutron star

    (due to deleptonization and neutrino diffusion)

  - convection inside neutrino heated hot bubble

    (behind shock wave due to neutrino energy deposition)

  - Rayleigh-Taylor instabilities in stellar envelope

    (due to non-steady shock propagation; triggered by hot bubble)

Numerical challenges (I): extreme range of scales both in time & space has to be treated properly

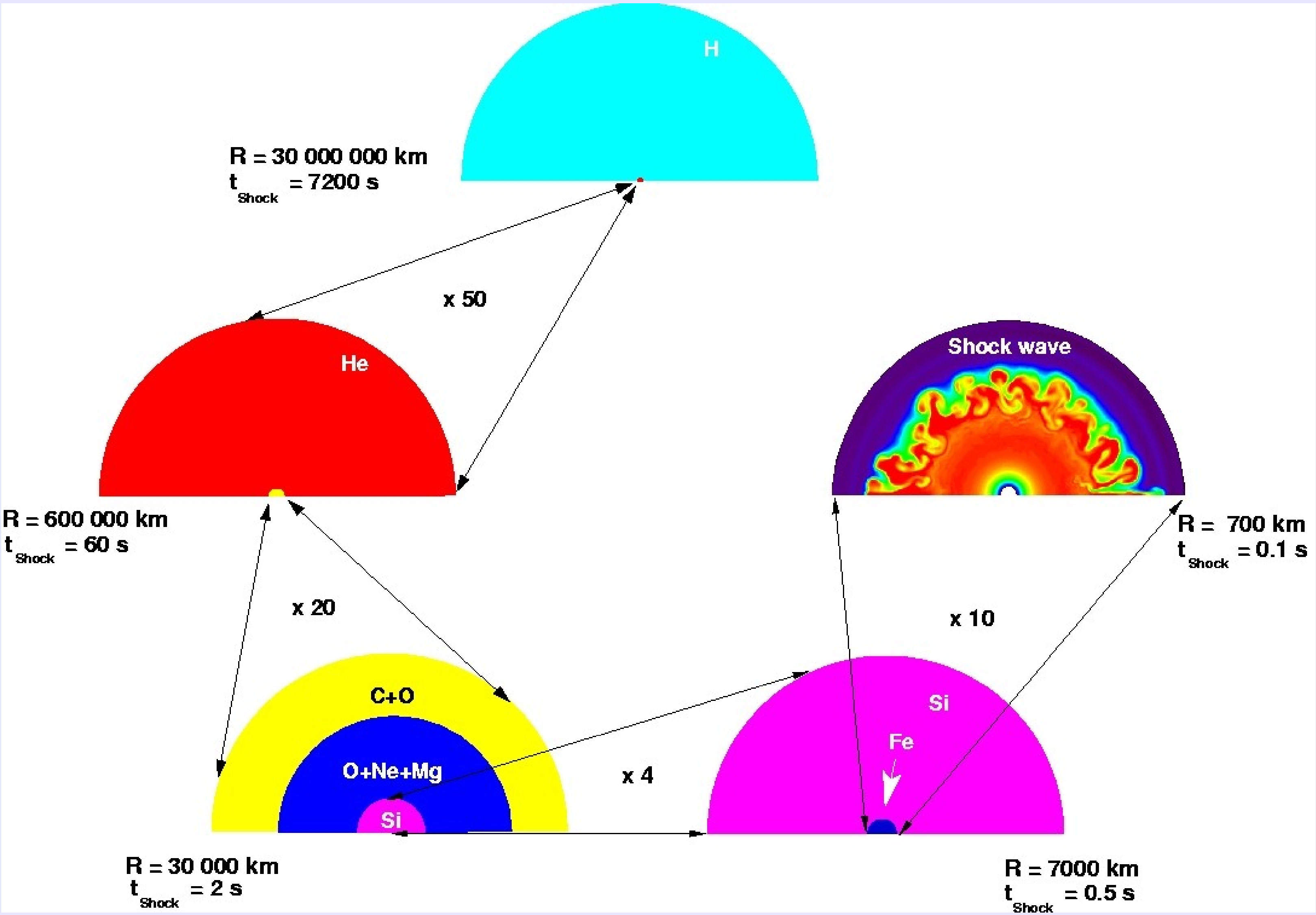

scale problem in CCSNe:

$l_{NS} \sim 10^{+6}$ cm

$l_{star} \sim 10^{+13}$ cm

$\tau_{NS} \sim 10^{-3}$ s

$\tau_{sh} \sim 10^{+4}$ s

--> factor 10^7

The Curse and Challenge of the Dimensions

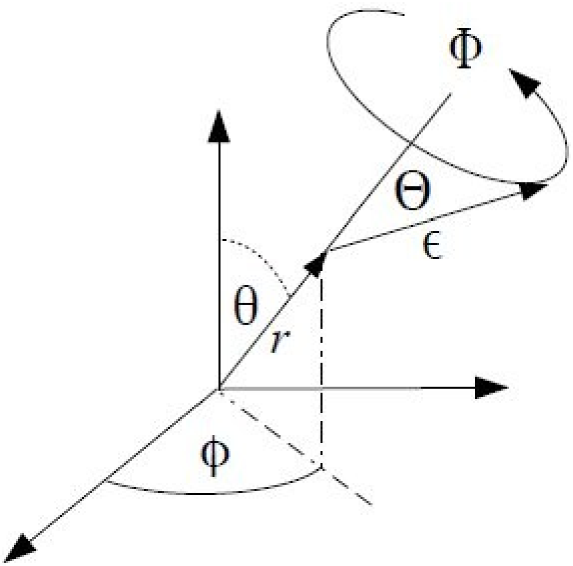

Boltzmann equation determines neutrino distribution function in 6D phase space and time

$$f(r, \theta, \phi, \Theta, \Phi, \epsilon, t)$$

Integration over 3D momentum space yields source terms for hydrodynamics

$$Q(r, \theta, \phi, t), \dot{Y}_e(r, \theta, \phi, t)$$

Solution approach	Required resources
• **3D** hydro + **6D** direct discretization of Boltzmann Eq. (code development by Sumiyoshi & Yamada '12)	• $\geq$ 10–100 PFlops/s (sustained!)
• **3D** hydro + two-moment closure of Boltzmann Eq. (may be next feasible step on way to full 3D)	• $\geq$ 1–10 Pflops/s, TBytes
• **3D** hydro + "**ray-by-ray-plus**" variable Eddington factor method (method used at MPA/Garching)	• $\geq$ 0.1–1 PFlops/s, Tbytes
• **2D** hydro + "**ray-by-ray-plus**" variable Eddington factor method (method used at MPA/Garching)	• $\geq$ 0.1–1 Tflops/s, < 1 TByte

courtesy of H-Th. Janka

Instabilities, mixing and nucleosynthesis in stellar envelope

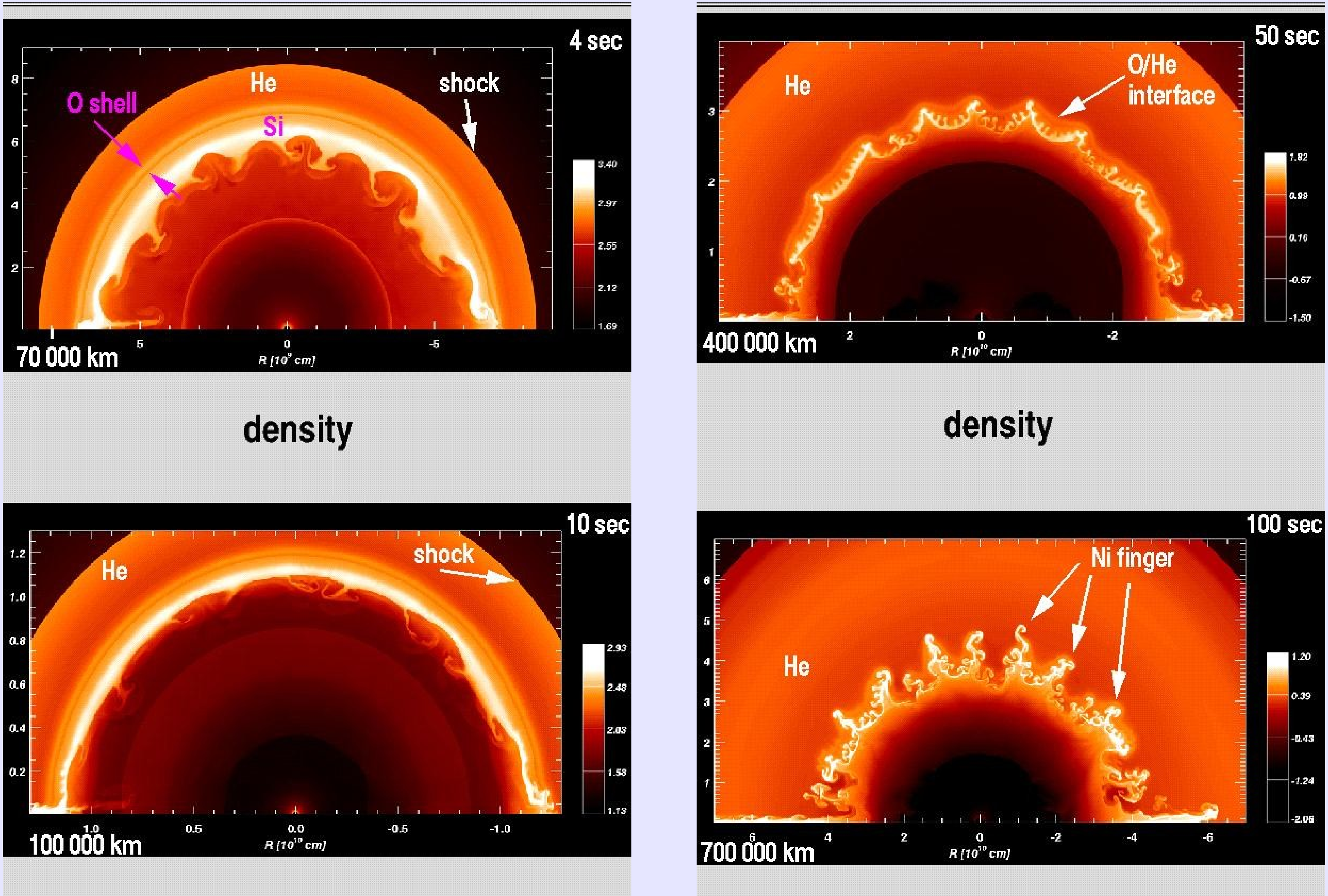

AMR simulation of shock propagation through stellar envelope (Kifonidis, Plewa, Janka & Müller 2003

Rayleigh-Taylor instabilities & mixing in stellar envelope

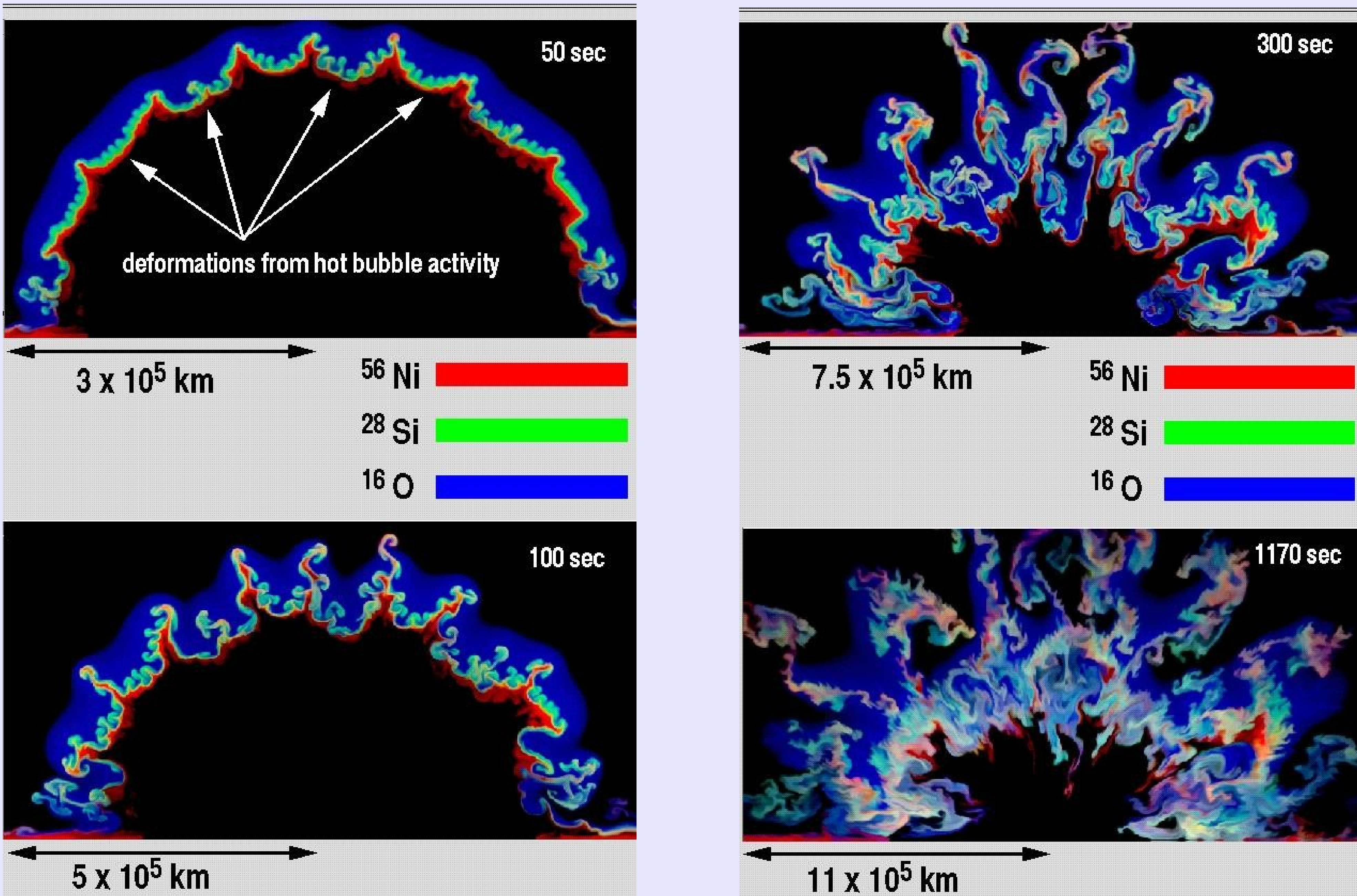

AMR simulation of shock propagation through stellar envelope (Kifonidis, Plewa, Janka & Müller 2003

Instabilities, mixing and nucleosynthesis in envelope

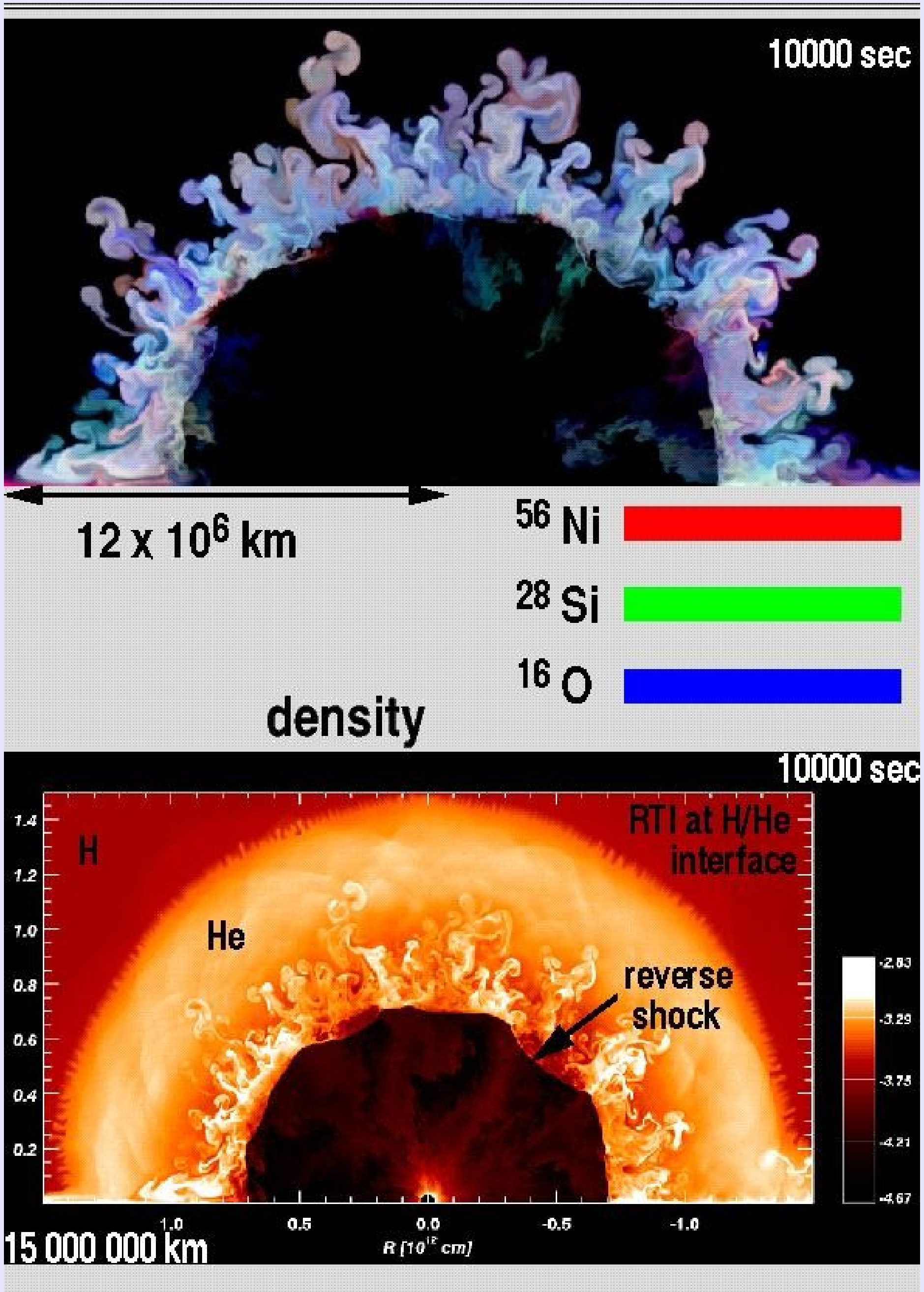

AMR simulation of shock propagation through stellar envelope
(Kifonidis, Plewa, Janka & Müller 2003

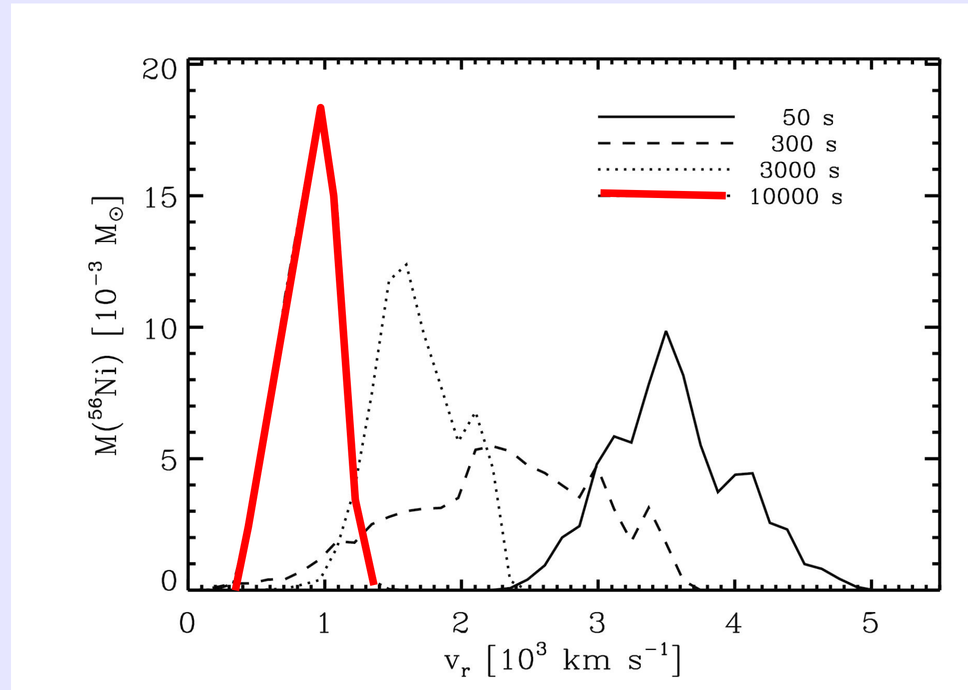

- results of simulations in accordance with observations of SNe Ib/Ic

- simulations do not reproduce large velocities of Fe/Ni observed in SN 1987A

Entropy-isosurfaces (left) of the SN shock (grey) & high-entropy bubbles (green), and entropy distribution in a cross-sectional plane (right)

NS accelerates due to asymmetric distribution of the ejecta

ejecta distribution becomes dipolar with more dense, low-entropy matter concentrated in hemisphere of kick direction

essentially spherically symmetric neutrino wind bubble develops

Wongwathanarat, Janka & Müller ApJL 725 ('10) 106; arXiv:1210.8148 ('12)

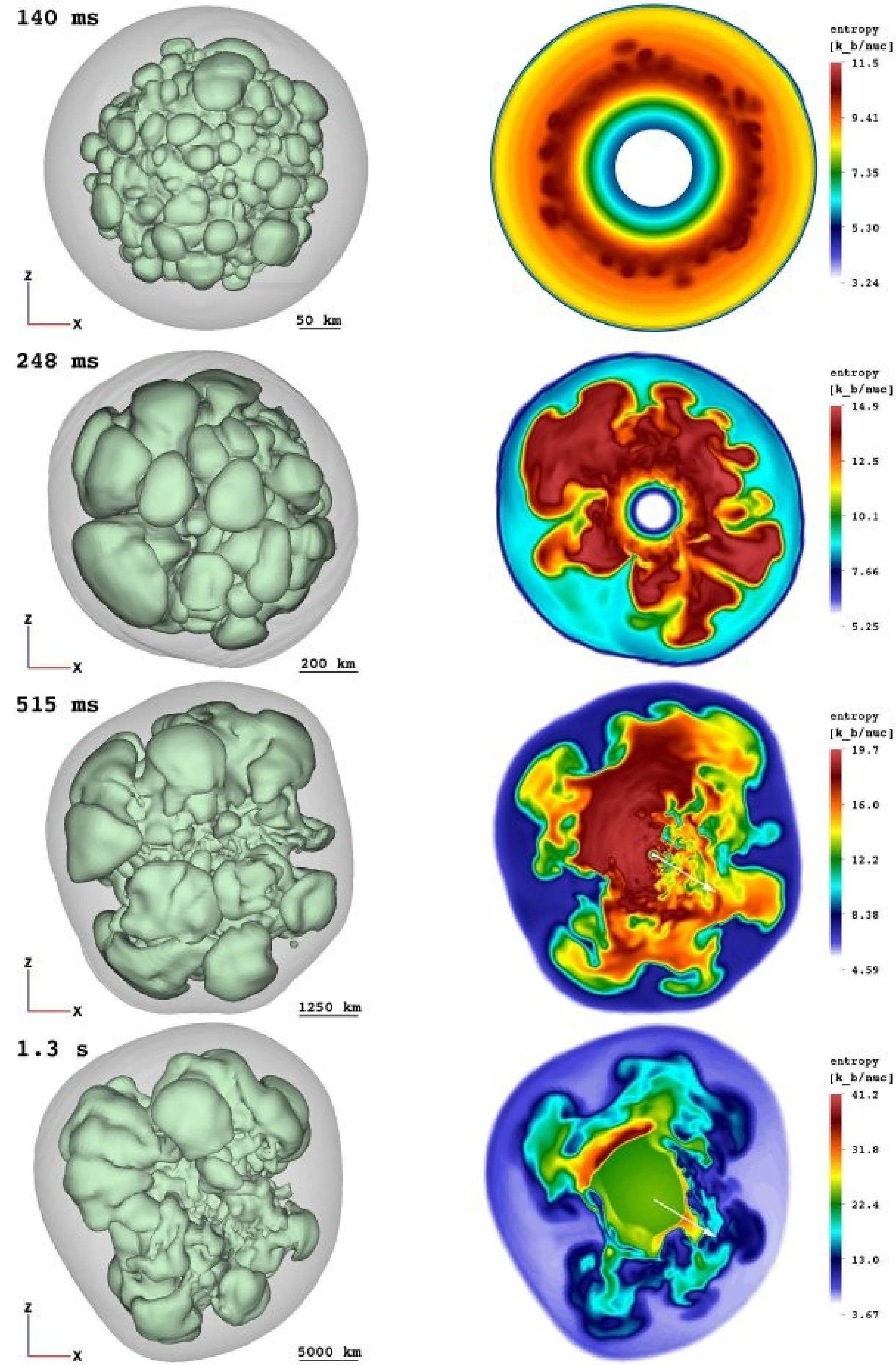

SN shock & bubbles *ray-casting images of the density* *entropy distribution*

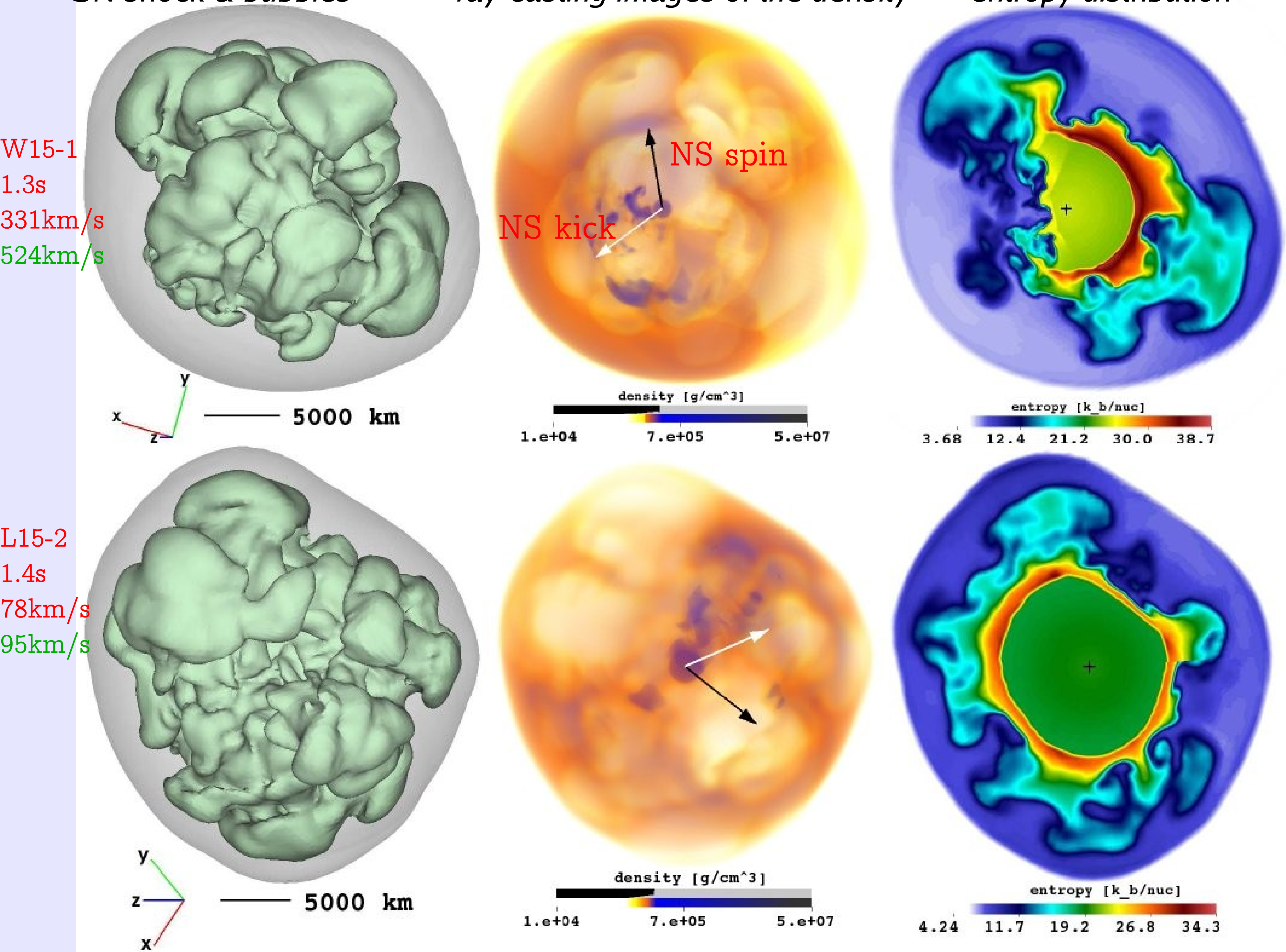

Wongwathanarat, Janka & Müller ApJL 725 (2010) 106; arXiv:1210.8148 (2012)

neutron star recoil by gravitational tug-boat mechanism

ejecta morphology of high kick models (575 km/s)

red:
high density clumps

beige & blue surfaces:
outer & inner boundary of inner ejecta

outermost surface:
SN shock

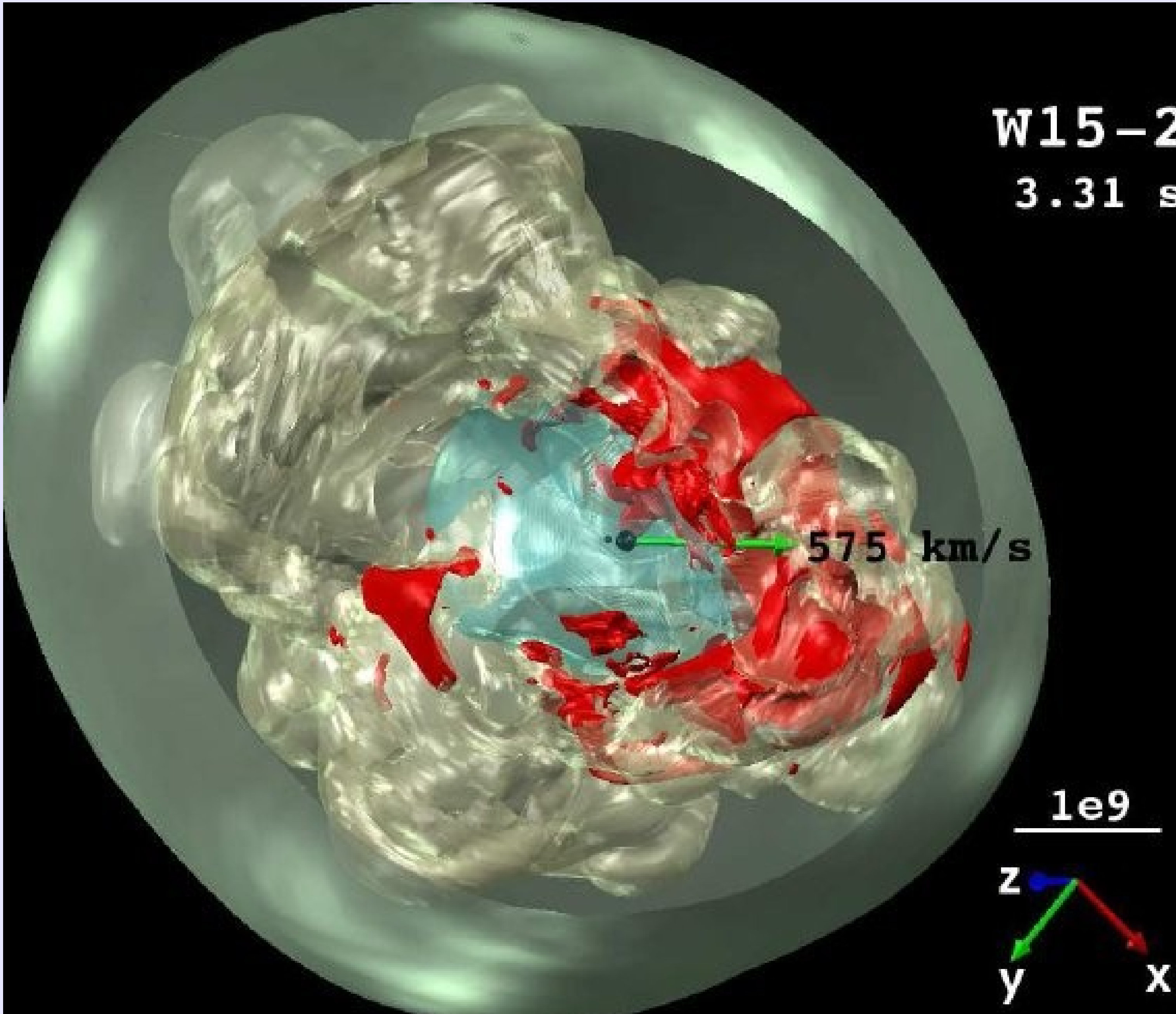

Wongwathanarat, Janka & Müller ApJL 725 (2010) 106; arXiv:1210.8148 (2012)

Explosion and NS properties for all simulated 3D models

				1.1 - 1.4 s				3.1 - 3.4 s				
Model	M_{ns} $[M_\odot]$	t_{exp} [ms]	E_{exp} [B]	v_{ns} [km/s]	a_{ns} [km/s^2]	$v_{ns,\nu}$ [km/s]	$\alpha_{k\nu}$ [°]	v_{ns}^{long} [km/s]	a_{ns}^{long} [km/s^2]	$J_{ns,46}$ [10^{46} g cm^2/s]	α_{sk} [°]	T_{spin} [ms]
W15-1	1.37	246	1.12	331	167	2	151	524	44	1.51	117	652
W15-2	1.37	248	1.13	405	133	1	126	575	49	1.56	58	632
W15-3	1.36	250	1.11	267	102	1	160	-	-	1.13	105	864
W15-4	1.38	272	0.94	262	111	4	162	-	-	1.27	43	785
W15-5-lr	1.41	289	0.83	373	165	2	129	-	-	1.63	28	625
W15-6	1.39	272	0.90	437	222	2	136	704	71	0.97	127	1028
W15-7	1.37	258	1.07	215	85	1	81	-	-	0.45	48	2189
W15-8	1.41	289	0.72	336	168	3	160	-	-	4.33	104	235
L15-1	1.58	422	1.13	161	69	5	135	227	16	1.89	148	604
L15-2	1.51	382	1.74	78	14	1	150	95	4	1.04	62	1041
L15-3	1.62	478	0.84	31	27	1	51	-	-	1.55	123	750
L15-4-lr	1.64	502	0.75	199	123	4	120	-	-	1.39	93	846
L15-5	1.66	516	0.62	267	209	3	147	542	106	1.72	65	695
N20-1-lr	1.40	311	1.93	157	42	7	118	-	-	5.30	122	190
N20-2	1.28	276	3.12	101	12	4	159	-	-	7.26	43	127
N20-3	1.38	299	1.98	125	15	5	138	-	-	4.42	54	225
N20-4	1.45	334	1.35	98	18	1	98	125	9	2.04	45	512
B15-1	1.24	164	1.25	92	16	1	97	102	1	1.03	155	866
B15-2	1.24	162	1.25	143	37	1	140	-	-	0.12	162	7753
B15-3	1.26	175	1.04	85	19	1	24	99	3	0.44	148	2050

Wongwathanarat, Janka & Müller ApJL 725 (2010) 106; arXiv:1210.8148 (2012) prediction of an observable fingerprint (in case of high kicks):

Ni production enhanced in direction of stronger explosion

i.e. opposite to NS kick direction (black arrow)!

model W15-2

Wongwathanarat, Janka & Müller ApJL 725 (2010) 106; arXiv:1210.8148 (2012)

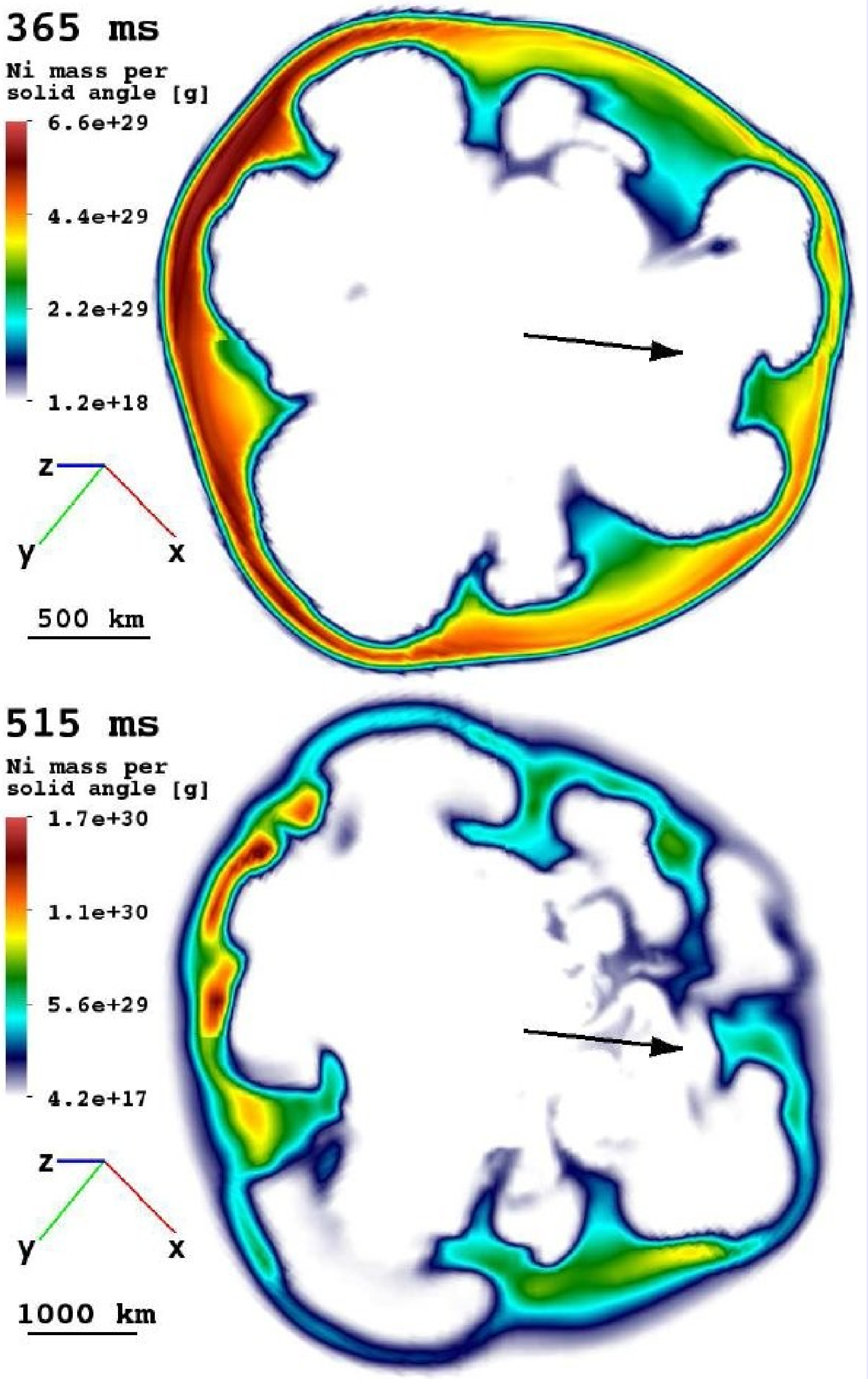

Hemispheric ejecta yields for the high-kick models W15-1/2 & moderate-kick models L15-1/2

Tracer: yield of Fe-group nuclei in neutrino-processed ejecta, some undertemined fraction of which may be ^{56}Ni

Model	^{4}He [$M_\odot$]		^{12}C [10^{-1} $M_\odot$]		^{16}O [10^{-1} $M_\odot$]		^{20}Ne [10^{-2} $M_\odot$]		^{24}Mg [10^{-2} $M_\odot$]	
	North	South	North	South	North	South	North	South	North	South
W15-1	2.78	2.66	1.18	1.10	3.68	3.75	8.90	8.49	2.41	2.85
W15-2	2.78	2.65	1.16	1.12	3.43	3.84	8.67	8.49	2.16	2.86
L15-1	2.39	2.34	0.90	0.87	2.77	2.89	5.00	5.06	2.12	2.49
L15-2	2.40	2.39	0.89	0.87	2.85	2.79	5.21	4.88	2.47	2.42

Model	^{28}Si [10^{-2} $M_\odot$]		^{40}Ca [10^{-2} $M_\odot$]		^{44}Ti [10^{-3} $M_\odot$]		^{56}Ni [10^{-2} $M_\odot$]		Tracer [10^{-2} $M_\odot$]	
	North	South	North	South	North	South	North	South	North	South
W15-1	1.88	2.92	1.33	4.81	0.68	2.43	1.26	4.28	2.23	6.08
W15-2	1.74	2.83	1.27	4.66	0.81	2.17	1.37	4.09	2.22	6.27
L15-1	1.75	2.33	1.76	2.47	1.49	2.40	1.34	1.87	4.78	7.20
L15-2	2.13	2.15	2.54	2.74	2.32	2.55	1.81	1.89	8.68	9.74

Wongwathanarat, Janka & Müller ApJL 725 (2010) 106; arXiv:1210.8148 (2012)

Neutron Star Recoil and Nickel Production

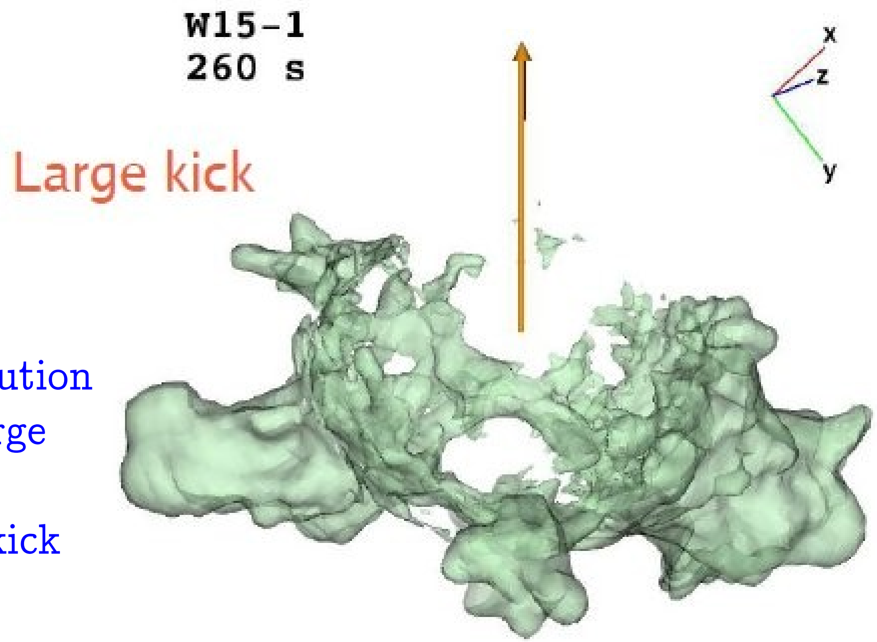

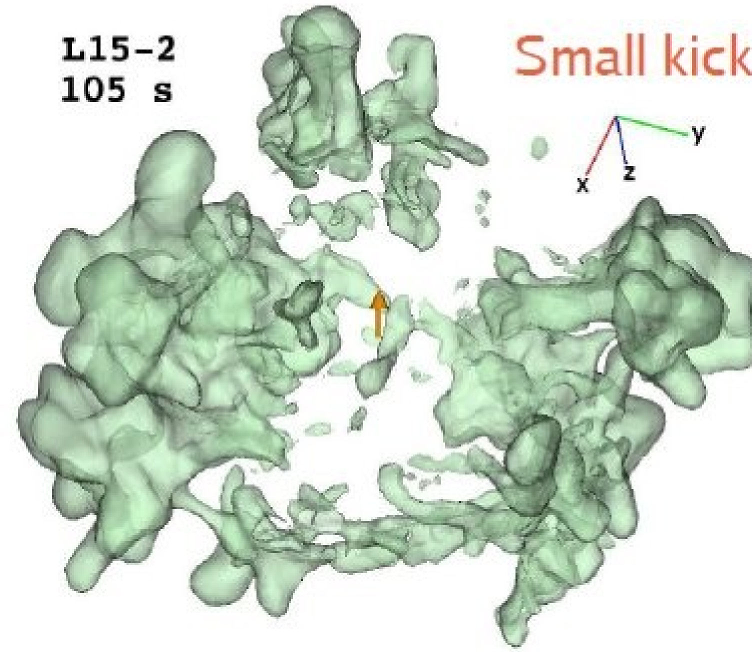

nickel distribution of a large and small kick model

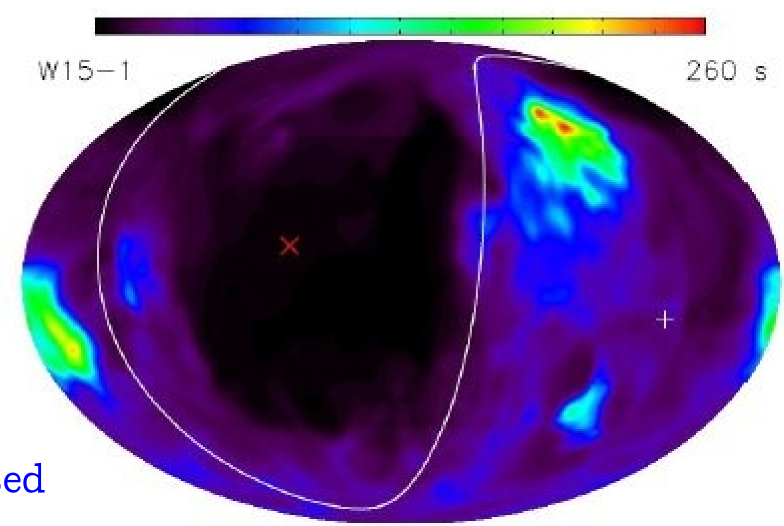

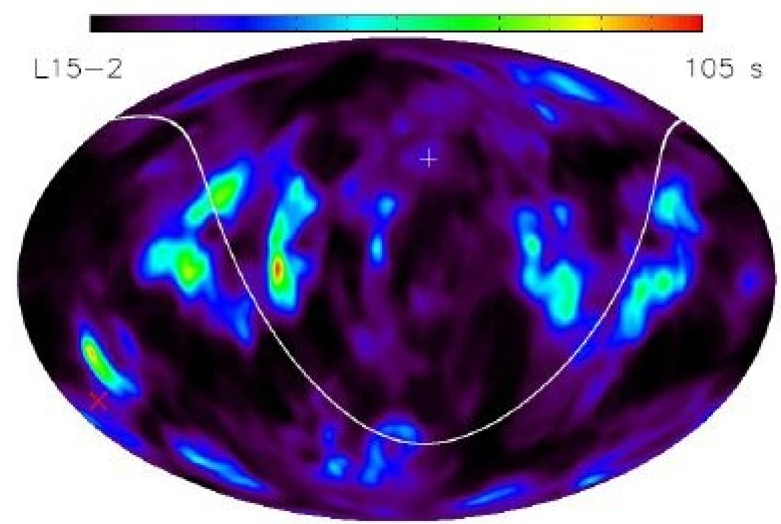

4π maps of the integrated nickel mass per solid angle

Wongwathanarat, Janka & Müller ApJL 725 (2010) 106; arXiv:1210.8148 (2012)

conclusions

non-radial flow and early mixing occurs in 2D/3D core-collapse supernova models because of

- neutrino-driven hydrodynamic instabilities in the supernova engine (producing NS kicks, and spins)

- shock-induced Rayleigh-Taylor instabilities in the stellar envelope

open questions

- dependence on explosion energy, progenitor, 2D/3D modeling?

- relative importance and interplay of the neutrino-driven and shock-induced instabilities?

- can we deduce from observations of young supernova remnants the operation of the supernova engine?

- influence of (rapid) rotation and (strong) magnetic fields?